Functional analyses of sirtuin in *Lactobacillus paracasei*

2016

Hotaka Atarashi

CONTENTS

CHAPTER 4
Intracellular localization of sirtuin protein in *L. paracasei* BL23

INTRODUCTION

Sirtuin was originally designated as silent information regulator 2 (SIR2) in yeast which stands for the silence regulation of mating type genes (Fritze et al., 1997). In addition, the main enzyme activity of sirtuin family proteins were proven that it was a NAD^+-dependent deacetylase (Imai et al., 2000). The sirtuin gene has begun to draw wider attention when it showed positive function in life span control (Anderson et al., 2003; Guarente and Kenyon, 2000; Lin et al., 2000). The similar effect on life span elongation has been demonstrated with nematode, fruit fly, yeast and mammalian cells by molecular approaches (Cohen et al., 2004; Kanfi et al., 2012; Saka et al., 2013). After the research was extended to mammalian system, it has been shown to involve in the regulation of metabolism, circadian rhythm and genetic stability, and the key downstream control point was unraveled to be TOR-mediated signal transduction (Blagosklonny, 2010; Guarente and Kenyon, 2000). Evolutional function of sirtuin was postulated to play a role in survival upon starvation, partly because its expression was shown to be up-regulated upon calorie restriction (Cohen et al., 2004). Previously, the author's group demonstrated that SIR3 and SIR4 deficiency in yeast resulted in improved resistance to ethanol and hydrogen peroxide (Matsuda et al., 2011). The gene sequences of bacterial sirtuin-homologs have been accumulated in the GenBank, providing a long list of bacterial sirtuins in many archaea- and eu-bacteria (Frye, 2000). As for the function of these putative ancestral sirtuin homologs, only a few cases have been reported. In *Escherichia coli* and in *Salmonella enterica*, it has been shown to deacetylate acetyl CoA synthetase, thereby activating the enzyme (Starai et al., 2002). While in *Bacillus subtilis*, two deacetylases either requiring or not-requiring NAD^+ are involved in the deacetylation

of the enzyme (Gardner et al., 2009; Gardner et al., 2006). In *E. coli* the chemotactic gene *cheY* product was reported to be deacetylated by CobB protein (Li et al., 2010). It is not clear whether bacterial sirtuin has a function similar in chromatin remodeling system in eukaryotes. However, as an example of individual transcription factor, it was reported that when the acetylated Lysine 180 of RcsB protein (two-component response regulator) was deacetylated by CobB protein, the DNA binding activity of RcsB is increased to activate transcription of the target gene, *flhDC* in *E. coli* (Thao et al., 2010). In addition, the importance of protein acetylation as a posttranslational modification has been documented as reviewed by others (Bernal et al., 2014). On the other hand, little is known about its roles in lactic acid bacteria (LAB). LAB are widely consumed by human as food fermentation starters and as probiotics.

There are a huge number of bacteria on the skin, and in intestinal and oral cavities. Above all, the intestinal bacteria inhabit at high density in the digestive canal. The intestinal bacteria produce essential amino acids, vitamin and short-chain fatty acids as metabolic end products useful to human. Whereas, several intestinal bacteria produce hydrogen sulfide and secondary bile acid as metabolic end products harmful to human. The change of the gut microbiota may cause disease such as allergy and type 2 diabetes in human (Clemente et al., 2012). The gut microbiota plays a major role in health and diseases in human. Therefore, probiotics as preventive medicine is important to maintain healthy homeostasis in human. Probiotics are live bacteria that are thought to be beneficial in preventing several health conditions. According to the 2002 definition by the World Health Organization (WHO), probiotics are “live microorganisms which, when administered in adequate amounts, confer a health benefit on the host.” (FAO/WHO Working Group. 2002). Therefore, those probiotics bacteria must be alive in probiotic

products before they were administered to the host. In addition, the important function of the probiotics was known to regulate of the functions of intestinal and immunopotentiative actions (Goldin et al., 2008). For example, *Lactobacillus rhamnosus* GG modify helps ameliorate allergic inflammation (Isolauri et al., 2000). *Lactobacillus gasseri* OLL 2716 (LG21) has suppressive effect on *Helicobacter pylori* infection in humans (Sakamoto et al., 2001) and bacteriocins produced by LAB kill or inhibit the growth of other unfavorable bacteria (Cleveland et al., 2001). The author thinks that it is an important subject to increase stress tolerance, adhesion to intestinal tract and production of the useful substances by LAB.

Therefore, the author assumed that it is important to increase stress tolerance, adhesion to intestinal tract and production of the useful substances by LAB in order to confer more beneficial health effects on the host. Based on these presumption, the author aimed to analyze the role of sirtuin in LAB.

In the chapters 1 and 2, the author analyzed sirtuin homolog genes of LAB, designated *sirA* and *sirB*. These genes cloned, and the corresponding recombinant proteins generated and purified for enzyme kinetics characterization. The purified recombinant LpSirA proteins displayed a comparable deacetylase activity with the recombinant human SIRT1. In the chapter 3, the author identified several candidate target proteins both *in vivo* and *in vitro* by using the recombinant LpSirA protein and sirtuin inhibitor nicotinamide (NAM) (Avalos et al., 2002). In the chapter 4, the author analyzed intracellular localization of sirtuin in *L. paracasei* by using immunofluorescence staining and LpSirA-Venus fusion protein.

CHAPTER 1
Identification of sirtuin genes in the genomes of the *L. paracasei* strains and its homology to sirtuins of related bacteria

1. INTRODUCTION

Yeast *sir2*-like gene was identified as one of the genes which controlled mating type of the *Saccharomyces cerevisiae* (Klar et al., 1979). Sirtuin was originally designated as silent information regulator 2 (SIR2) in yeast which stands for the silence regulation of mating type genes (Fritze et al., 1997). In addition, the main enzyme activity of sirtuin family proteins were proved that it was NAD^+-dependent deacetylase (Imai et al., 2000). Later, the function of sirtuin was reported with the prokaryote as well as eukaryote. The gene sequences of bacterial sirtuin-homologs have been accumulated in the GenBank, providing a long list of bacterial sirtuins in many archaea- and eu-bacteria (Frye, 2000; Hrschey et al., 2011). As for the function of these putative ancestral sirtuin homologs, only a few cases have been reported, for example, in *E. coli*, *S. enterica* and *B. subtilis*. However, it has not been reported the existence of sirtuin homolog gene and the function of sirtuin homolog protein in LAB. In a previous study, the author's group determined draft genome sequences of three *L. paracasei* strains isolated from either animal or plant origins with different cholate resistance (Shiwa et al., 2015).

In this chapter, the author demonstrated that the existence of sirtuin homolog gene in LAB by using GOLD program (DOE JGI-The U.S. Department of Energy Joint Genome Institute, Walnut Creek, CA, USA., https://gold.jgi.doe.gov/index). In addition, the author identified the sirtuin homolog of *L. paracasei* and compared it with sirtuins of

various species by using LALIGN program (EMBL-European Bioinformatics Institute, Hinxton, Cambridge, UK., http://www.ebi.ac.uk/Tools/psa/lalign/)..

2. MATERIALS AND METHODS

2.1 Identification of sirtuin genes in the genomes of the *L. paracasei* strains and its homology to sirtuins of related bacteria

Chemicals were of special grade unless otherwise mentioned. *Lactobacillus paracasei* strains NRIC 0644, NRIC 1917 and NRIC 1981 were obtained from NRIC culture collection (Tokyo University of Agriculture, Japan). Strains NRIC 1917 and NRIC 1981 were isolated from sugar cane wine and compost respectively, whereas origin of NRIC 0644 was unknown (Shiwa et al., 2015). The details of methodology and basic data of the genome analysis of the strains used in this work were published elsewhere (Shiwa et al., 2015). In this study, identification of sirtuin genes in the draft genomes was performed by using data analysis program, *In Silico* Molecular Cloning (*In Silico* Biotechnology, Yokohama, Japan). For sequence comparison at the level of amino acid sequence, the sequences obtained by determining individual cloned DNAs were used as described in the following section using an application program, Keyword Search, of the *In Silico* Molecular Cloning program.

The existence of sirtuin homolog gene in LAB was demonstrated by using GOLD program. Genomes Online Database (GOLD) is a World Wide Web resource for comprehensive access to information regarding genome and metagenome sequencing projects, and their associated metadata around the world. Using GOLD program, the author searched for sirtuin homolog genes from *Lactobacillus* spp. *Leuconostoc* spp.

Lactococcus spp. *Pediococcus* spp. *Streptococcus* spp. *Melissococcus* spp. *Enterococcus* spp. *Weissella* spp. *Carnobacterium* spp. *Atopobium* spp. *Tetragenococcus* spp. *Olsenella* spp. *Oenococcus* spp. and *Bifidobacterium* spp.

In addition, the amino acid sequence similarity values with other organisms were calculated by using LALIGN program.

2.2 Cloning of DNAs encoding sirtuin homolog

The three strains of *L. paracasei* were cultured in MRS broth at 37 ˚C overnight. Genomic DNA was extracted from the cells as described in the manufacturer's instruction in the DNeasy Blood & Tissue Kit (QIAGEN, Venlo, Netherlands). Based on the draft sequences of *L. paracasei* strains, primers (*sirA*-N and *sirA*-C, Table 1) were designed for amplification of sirtuin homolog gene. The amplified products were sub-cloned into pT7 Blue vector by TA cloning (Novagen Merck Millipore, Darmstadt, Germany) and transformed to DH5α (Nippon Gene Co., Ltd, Tokyo, Japan). DNA sequence of the cloned DNA was determined by analyzing dye-labeled extension products using BigDye® terminator v1.1 cycle sequencing kit (Applied Biosystems, Carlsbad, CA) subjected to a DNA sequencer 3100 Avant Genetic Analyzer (Applied Biosystems, Waltham, MA). The sequence data were determined following sequencing both directions of the DNAs. Sequencing and cloning primers are listed in the Table 1.

3. RESULTS AND DISCUSSION

3.1 Identification of sirtuin genes in the genomes of the *L. paracasei* strains and its homology to sirtuins of related bacteria

A homology search through GenBank data indicated that LAB and bifidobacteria have homologs of eukaryotic sirtuin, but not other hydrolase-types of protein deacetylase such as class I, II, and IV HDACs. HDACs has been classified in four classes in human, namely, class I HDACs (HDAC1, 2, 3 and 8), class II HDACs (HDAC4, 5, 6, 7, 9 and 10), class III HDACs (SIRT1-7) and class IV HDAC (HDAC11). Class III HDACs (sirtuin type) have been identified as SIR2 family of NAD^+-dependent deacetylase, and other HDACs have been identified as Zn^{2+}-dependent deacetylase (Gray et al., 2001; Ruijter et al., 2003). Interestingly, although the author found existence of the 1 to 8 sirtuin genes in almost all LAB species through data bank survey, the author was not able to find the sirtuin homolog genes in *Lactococcus* spp. *Carnobacterium* spp. and *Melissococcus* spp. (Table 2).

Within the draft genomes of three strains, a 693 base pair-long ORF coding for a 230 amino acid (aa)-long polypeptide, highly homologous to the deduced aa sequences based on the DNA sequence deposited as the *L. paracasei* sirtuin homolog was identified (99.9% homologous to those of *L. paracasei* BL23, NCBI-Gene ID:6407162). As the draft genome sequence information may not be accurate, the author next tried to clone individual DNAs to determine the sequences unambiguously.

3.2 Cloning of individual DNAs coding for sirtuin homolog from strains NRIC 0644, 1917 and 1981

The sirtuin homolog genes were directly cloned from DNA isolated from three strains by PCR cloning method and the sequences of the cloned DNA were determined by sequencing both directions as described in materials and methods.

Obtained DNA sequences were used to determine corresponding deduced amino

acid sequence which was then aligned using BioEdit Sequence Alignment Editor as shown in Fig. 1. Based on the deduced amino acid sequences, strains NRIC 0644 and NRIC 1917 were shown to have an ORF 99% homologous to that of strain *L. paracasei* BL23 (LCABL_27750, NCBI-Gene ID:6407162), while strain NRIC 1981 had an ORF 99 % homologous to that of strain *L. paracasei* Zhang (LCAZH_2574 NCBI-Gene ID:9460483). The author tentatively designated the gene as *sirA* (indicating the first sirtuin homolog of *L. paracasei*). Interestingly, there was another sirtuin isozyme found in the genome of strain NRIC 1981, which shared 78% identity with that of *L. rhamnosus* GG sirtuin (LGG_01347 NCBI-Gene ID: 8421081). The author designated this second gene as *sirB*, which was not found in the genomes of the strains NRIC 0644, and NRIC 1917.

The amino acid sequences of *sirA* genes from three strains were similar to each other. Two active histidine residue sites as reported in human SIRT1 (Sanders *et al*., 2009) were conserved in the clones of all three strains (his 327 and his 363 of SIRT1, which corresponded to his 79 and his 113 of LpSirA protein as indicated by single-headed arrows in Fig. 1). The NAD^+-binding motif, called Rossmann fold sequence, was also present in all three clones as marked by double-headed arrows in Fig. 1. When comparison was made using LALIGN program, the overall LpSirA sequence was 26.2% homologous to yeast Sir2 (BL23 LpSirA residues 8-226 vs *S. cerevisiae* Sir2 residues 251-518) and 29.4% homologous to human SIRT1 (BL23 LpSirA residues 3-208 vs SIRT1 residues 245-469). The LpSirB isolated from the strain NRIC 1981 contained similar NAD^+-binding domains, but only one conserved active histidine residue (his 79) site.

The amino acid sequence homology of LpSirA proteins with sirtuins of *E. coli*, *Salmonella enterica* serovar Typhimurium LT2 and *B. subtilis* were 29.3%, 29.5% and

31.1%, respectively, indicating LpSirA is not highly homologous to other bacterial sirtuins, even the homology between *E. coli* sirtuin and *S. enterica* serovar Typhimurium LT2 sirtuin was 91.9%. The amino acid sequence of LpSirB protein showed only 80% homology to other reported *L. rhamnosus* sirtuins which share 94-97 % homology with each other.

GenBank accession numbers of the *sirA* of NRIC 0644, NRIC 1917 and NRIC 1981 and *sirB* of NRIC 1981 are AB728561, AB728562, AB728563 and AB728564, respectively.

Table 1 PCR primers used in cloning and sequencing

Primer	5' to 3'	Restriction enzyme	Recognition sequence
sirA-N	ATGTTTGATCTGCAAACTGC		
sirA-C	TCAGACTACCAGCTTCGCAAATA		
sirB-N	ATGAAACAAAAGCAACGTTTGC		
sirB-C	TCACGCTATGATGCTGCTG		
CCTA-*Xho* I-*sirA*-N	CCTACTCGAGATGTTTGATCTGCAAACTGC	*Xho* I	CTCGAG
GATC-*Bpu*1102 I-*sirA*-C	GATCGCTCAGCTCAGACTACCAGCTTCGCA	*Bpu*1102 I	GCTCAGC
CCTA-*Xho* I-*sirB*-N	CCTACTCGAGATGAAACAAAAGCAACGTTTGC	*Xho* I	CTCGAG
GATC-*Bpu*1102 I-*sirB*-C	GATCGCTCAGCTCACGCTATGATGCTGCTG	*Bpu*1102 I	GCTCAGC
sirA-151	GATAATTTACAAGCACATCA		
sirA-170	TGATGTGCTTGTAAATTATC		
sirA-531	GGTGGGAACAAGCTTCGTGG		
sirA-550	CCACGAAGCTTGTTCCCACC		
sirA-NRIC0644-235	ATGGTTGCCATTTTCTCGTG		
sirA-NRIC0644-578	ATGCGCAACCAGAGGCGACC		
sirA-NRIC1917-101	ATCGGCGTATAGCCCGCCCT		
sirA-NRIC1981-211	ACGTTCGGTTTAGCCGCTGG		
sirA-NRIC1981-281	CGCAGAATGTTGACGGCCTC		
sirA-NRIC1981-551	TTTATCCATTTGCGGGGTTG		
sirB-NRIC1981-100	TCCCTGATTCAGTCGAGATA		
sirB-NRIC1981-150	AAACTTGTGTGATTTGTGTA		
sirB-NRIC1981-231	TTTCTGTCAACCCAAGGCAC		
sirB-NRIC1981-250	GTGCCTTGGGTTGACAGAAA		
sirB-NRIC1981-472	GGATTGATTTTACCCGATTT		
sirB-NRIC1981-491	AAATCGGGTAAAATCAATCC		

Underlines indicate artificially added sequences corresponding to the recognition sites of the restriction enzymes listed herein.

Table 2 Ratio of sirtuin harboring strains in a variety of LAB species

Species	Ratio		Species	Ratio
Lactobacillus acetotolerans	1/1		*Enterococcus casseliflavus*	1/1
Lactobacillus acidophilus	4/4		*Enterococcus durans*	0/2
Lactobacillus amylovorus	2/2		*Enterococcus faecalis*	7/7
Lactobacillus brevis	2/2		*Enterococcus faecium*	5/5
Lactobacillus buchneri	2/2		*Enterococcus hirae*	1/1
Lactobacillus casei	1/1		*Enterococcus mundtii*	1/1
Lactobacillus crispatus	1/1		*Enterococcus sp*	1/1
Lactobacillus delbrueckii	4/4			
Lactobacillus fermentum	4/4		*Leuconostoc carnosum*	1/1
Lactobacillus gasseri	2/2		*Leuconostoc citreum*	1/1
Lactobacillus ginsenosidimutans	1/1		*Leuconostoc gasicomitatum*	1/1
Lactobacillus helveticus	7/7		*Leuconostoc gelidum*	1/1
Lactobacillus hokkaidonensis	1/1		*Leuconostoc kimchii*	1/1
Lactobacillus johnsonii	4/4		*Leuconostoc mesenteroides*	4/4
Lactobacillus kefiranofaciens	1/1		*Leuconostoc sp*	1/1
Lactobacillus koreensis	1/1			
Lactobacillus paracasei	10/10		*Weissella ceti*	0/3
Lactobacillus plantarum	9/9		*Weissella cibaria*	1/1
Lactobacillus reuteri	5/5		*Weissella koreensis*	0/1
Lactobacillus rhamnosus	6/6			
Lactobacillus ruminis	1/1		*Oenococcus oeni*	1/1
Lactobacillus sakei	1/1		*Oenococcus kitaharae*	1/1
Lactobacillus salivarius	4/4			
Lactobacillus sanfranciscensis	1/1		*Pediococcus claussenii*	1/1
Lactobacillus sp	2/2		*Pediococcus pentosaceus*	0/2
Streptococcus mutans	0/5		*Carnobacterium maltaromaticum*	0/1
Streptococcus oligofermentans	1/1		*Carnobacterium sp*	0/2
Streptococcus oralis	0/1			
Streptococcus parasanguinis	2/2		*Atopobium parvulum*	1/1
Streptococcus parauberis	0/1			
Streptococcus pasteurianus	0/1		*Tetragenococcus halophilus*	1/1
Streptococcus pneumoniae	0/26			
Streptococcus pseudopneumoniae	0/1		*Olsenella uli*	2/2
Streptococcus pyogenes	23/31			
Streptococcus salivarius	1/3		*Bifidobacterium actinocoloniiforme*	1/1
Streptococcus sanguinis	0/1		*Bifidobacterium adolescentis*	3/3
Streptococcus sp	3/3		*Bifidobacterium animalis*	14/14
Streptococcus suis	3/23		*Bifidobacterium asteroides*	1/1
Streptococcus thermophilus	0/10		*Bifidobacterium bifidum*	3/3
Streptococcus uberis	0/1		*Bifidobacterium breve*	6/6
			Bifidobacterium coryneforme	1/1
Lactococcus garvieae	0/2		*Bifidobacterium dentium*	1/1
Lactococcus lactis	0/14		*Bifidobacterium kashiwanohense*	1/1
			Bifidobacterium longum	13/13
Melissococcus plutonius	0/2		*Bifidobacterium pseudolongum*	1/1
			Bifidobacterium thermophilum	1/1

The denominator shows the number of bacterial species strains that are registered in the GOLD program. The numerator shows the number of bacterial species strains which have sirtuin homolog gene (s) as of 2016.

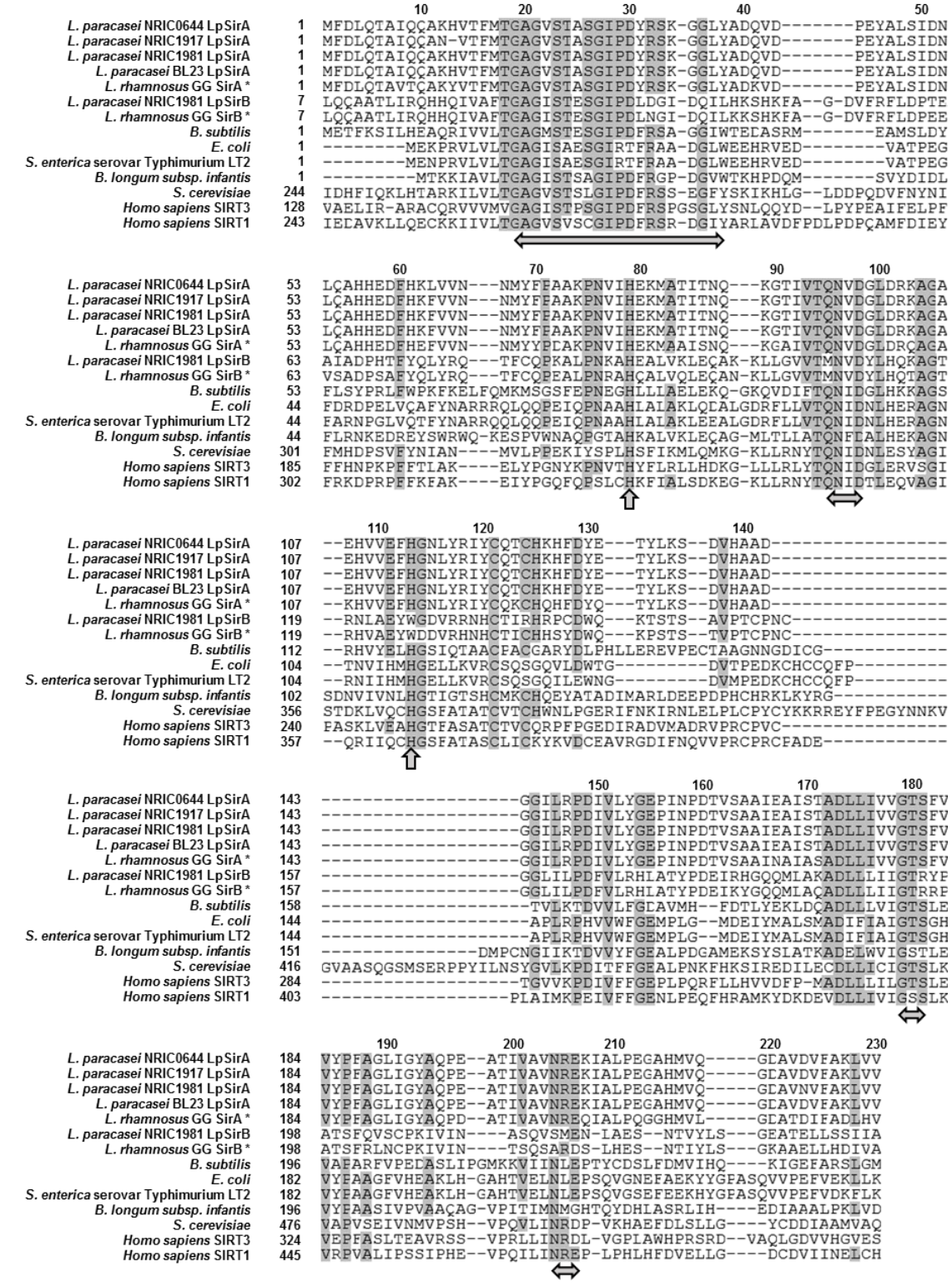
10 20 30 40 50
L. paracasei NRIC0644 LpSirA 1 MFDLQTAIQQAKHVTFMTGAGVSTASGIPDYRSK-GGLYADQVD-------PEYALSIDN
L. paracasei NRIC1917 LpSirA 1 MFDLQTAIQQAN-VTFMTGAGVSTASGIPDYRSK-GGLYADQVD-------PEYALSIDN
L. paracasei NRIC1981 LpSirA 1 MFDLQTAIQQAKHVTFMTGAGVSTASGIPDYRSK-GGLYADQVD-------PEYALSIDN
L. paracasei BL23 LpSirA 1 MFDLQTAIQQAKHVTFMTGAGVSTASGIPDYRSK-GGLYADQVD-------PEYALSIDN
L. rhamnosus GG SirA * 1 MFDLQTAVTQAKYVTFMTGAGVSTASGIPDYRSK-GGLYADKVD-------PEYALSIDN
L. paracasei NRIC1981 LpSirB 7 LQQAATLIRQHHQIVAFTGAGISTESGIPDLDGI-DQILHKSHKFA--G-DVFRFLDPTE
L. rhamnosus GG SirB * 7 LQQAATLIRQHHQIVAFTGAGISTESGIPDLNGI-DQILKKSHKFA--G-DVFRFLDPEE
B. subtilis 1 METFKSILHEAQRIVVLTGAGMSTESGIPDFRSA-GGIWTEDASRM-------EAMSLDY
E. coli 1 --------MEKPRVLVLTGAGISAESGIRTFRAA-DGLWEEHRVED--------VATPEG
S. enterica serovar Typhimurium LT2 1 --------MENPRVLVLTGAGISAESGIRTFRAA-DGLWEEHRVED--------VATPEG
B. longum subsp. infantis 1 ---------MTKKIAVLTGAGISTSAGIPDFRGP-DGVWTKHPDQM-------SVYDIDL
S. cerevisiae 244 IDHFIQKLHTARKILVLTGAGVSTSLGIPDFRSS-EGFYSKIKHLG--LDDPQDVFNYNI
Homo sapiens SIRT3 128 VAELIR-ARACQRVVVMVGAGISTPSGIPDFRSPGSGLYSNLQQYD--LPYPEAIFELPF
Homo sapiens SIRT1 243 IEDAVKLLQECKKIIVLTGAGVSVSCGIPDFRSR-DGIYARLAVDFPDLPDPQAMFDIEY
60 70 80 90 100
L. paracasei NRIC0644 LpSirA 53 LQAHHEDFHKLVVN---NMYFFAAKPNVIHEKMATITNQ---KGTIVTQNVDGLDRKAGA
L. paracasei NRIC1917 LpSirA 53 LQAHHEDFHKFVVN---NMYFFAAKPNVIHEKMATITNQ---KGTIVTQNVDGLDRKAGA
L. paracasei NRIC1981 LpSirA 53 LQAHHEDFHKFVVN---NMYFFAAKPNVIHEKMATITNQ---KGTIVTQNVDGLDRKAGA
L. paracasei BL23 LpSirA 53 LQAHHEDFHKFVVN---NMYFFAAKPNVIHEKMATITNQ---KGTIVTQNVDGLDRKAGA
L. rhamnosus GG SirA * 53 LQAHHEDFHEFVVN---NMYYPLAKPNVIHEKMAAISNQ---KGAIVTQNVDGLDRQAGA
L. paracasei NRIC1981 LpSirB 63 AIADPHTFYQLYRQ---TFCQPKALPNKAHEALVKLEQAK-KLLGVVTMNVDYLHQKAGT
L. rhamnosus GG SirB * 63 VSADPSAFYQLYRQ---TFCQPEALPNRAHQALVQLEQAN-KLLGVVTMNVDYLHQTAGT
B. subtilis 53 FLSYPRLFWPKFKELFQMKMSGSFEPNEGHLLLAELEKQ-GKQVDIFTQNIDGLHKKAGS
E. coli 44 FDRDPELVQAFYNARRRQLQQPEIQPNAAHLALAKLQDALGDRFLLVTQNIDNLHERAGN
S. enterica serovar Typhimurium LT2 44 FARNPGLVQTFYNARRQQLQQPEIQPNAAHLALAKLEEALGDRFLLVTQNIDNLHERAGN
B. longum subsp. infantis 44 FLRNKEDREYSWRWQ-KESPVWNAQPGTAHKALVKLEQAG-MLTLLATQNFDALHEKAGN
S. cerevisiae 301 FMHDPSVFYNIAN----MVLPPEKIYSPLHSFIKMLQMKG-KLLRNYTQNIDNLESYAGI
Homo sapiens SIRT3 185 FFHNPKPFFTLAK----ELYPGNYKPNVTHYFLRLLHDKG-LLLRLYTQNIDGLERVSGI
Homo sapiens SIRT1 302 FRKDPRPFFKFAK----EIYPGQFQPSLCHKFIALSDKEG-KLLRNYTQNIDTLEQVAGI
110 120 130 140
L. paracasei NRIC0644 LpSirA 107 --EHVVEFHGNLYRIYCQTCHKHFDYE---TYLKS--DVHAAD----------------
L. paracasei NRIC1917 LpSirA 107 --EHVVEFHGNLYRIYCQTCHKHFDYE---TYLKS--DVHAAD----------------
L. paracasei NRIC1981 LpSirA 107 --EHVVEFHGNLYRIYCQTCHKHFDYE---TYLKS--DVHAAD----------------
L. paracasei BL23 LpSirA 107 --EHVVEFHGNLYRIYCQTCHKHFDYE---TYLKS--DVHAAD----------------
L. rhamnosus GG SirA * 107 --KHVVEFHGNLYRIYCQKCHQHFDYQ---TYLKS--DVHAAD----------------
L. paracasei NRIC1981 LpSirB 119 --RNLAEYWGDVRRNHCTIRHRPCDWQ---KTSTS--AVPTCPNC---------------
L. rhamnosus GG SirB * 119 --RHVAEYWDDVRHNHCTICHHSYDWQ---KPSTS--TVPTCPNC---------------
B. subtilis 112 --RHVYELHGSIQTAACPACGARYDLPHLLEREVPECTAAGNNGDICG-----------
E. coli 104 --TNVIHMHGELLKVRCSQSGQVLDWTG---------DVTPEDKCHCCQFP---------
S. enterica serovar Typhimurium LT2 104 --RNIIHMHGELLKVRCSQSGQILEWNG---------DVMPEDKCHCCQFP---------
B. longum subsp. infantis 102 SDNVIVNLHGTIGTSHCMKCHQEYATADIMARLDEEPDPHCHRKLKYRG-----------
S. cerevisiae 356 STDKLVQCHGSFATATCVTCHWNLPGERIFNKIRNLELPLCPYCYKKRREYFPEGYNNKV
Homo sapiens SIRT3 240 FASKLVEAHGTFASATCTVCQRPFPGEDIRADVMADRVPRCPVC----------------
Homo sapiens SIRT1 357 --QRIIQCHGSFATASCLICKYKVDCEAVRGDIFNQVVPRCPRCPADE------------
150 160 170 180
L. paracasei NRIC0644 LpSirA 143 --------------------GGILRPDIVLYGEPINPDTVSAAIEAISTADLLIVVGTSFV
L. paracasei NRIC1917 LpSirA 143 --------------------GGILRPDIVLYGEPINPDTVSAAIEAISTADLLIVVGTSFV
L. paracasei NRIC1981 LpSirA 143 --------------------GGILRPDIVLYGEPINPDTVSAAIEAISTADLLIVVGTSFV
L. paracasei BL23 LpSirA 143 --------------------GGILRPDIVLYGEPINPDTVSAAIEAISTADLLIVVGTSFV
L. rhamnosus GG SirA * 143 --------------------GGILRPDIVLYGEPINPDTVSAAINAIASADLLIVVGTSFV
L. paracasei NRIC1981 LpSirB 157 --------------------GGLILPDFVLRHLATYPDEIRHGQQMLAKADLLLIIGTRYP
L. rhamnosus GG SirB * 157 --------------------GGLILPDFVLRHLATYPDEIKYGQQMLAQADLLLIIGTRRP
B. subtilis 158 --------------------TVLKTDVVLFGLAVMH--FDTLYEKLDQADLLLVIGTSLE
E. coli 144 --------------------APLRPHVVWFGEMPLG--MDEIYMALSMADIFIAIGTSGH
S. enterica serovar Typhimurium LT2 144 --------------------APLRPHVVWFGEMPLG--MDEIYMALSMADIFIAIGTSGH
B. longum subsp. infantis 151 ----------------DMPCNGIIKTDVVYFGEALPDGAMEKSYSLATKADELWVIGSTLE
S. cerevisiae 416 GVAASQGSMSERPPYILNSYGVLKPDITFFGEALPNKFHKSIREDILECDLLICIGTSLK
Homo sapiens SIRT3 284 --------------------TGVVKPDIVFFGEPLPQRFLLHVVDFP-MADLLLILGTSLE
Homo sapiens SIRT1 403 --------------------PIAIMKPEIVFFGENLPEQFHRAMKYDKDEVDLLIVIGSSLK
190 200 210 220 230
L. paracasei NRIC0644 LpSirA 184 VYPFAGLIGYAQPE--ATIVAVNREKIALPEGAHMVQ-----GDAVDVFAKLVV
L. paracasei NRIC1917 LpSirA 184 VYPFAGLIGYAQPE--ATIVAVNREKIALPEGAHMVQ-----GDAVDVFAKLVV
L. paracasei NRIC1981 LpSirA 184 VYPFAGLIGYAQPE--ATIVAVNREKIALPEGAHMVQ-----GDAVNVFAKLVV
L. paracasei BL23 LpSirA 184 VYPFAGLIGYAQPE--ATIVAVNREKIALPEGAHMVQ-----GDAVDVFAKLVV
L. rhamnosus GG SirA * 184 VYPFAGLIGYAQPD--ATIVAVNREQIALPQGGHMVL-----GDATDIFADLHV
L. paracasei NRIC1981 LpSirB 198 ATSFQVSCPKIVIN----ASQVSMEN-IAES--NTVYLS---GEATELLSSIIA
L. rhamnosus GG SirB * 198 ATSFRLNCPKIVIN----TSQSARDS-LHES--NTIYLS---GKAAELLHDIVA
B. subtilis 196 VAFARFVPELASLIPGMKKVIINLEPTYCDSLFDMVIHQ----KIGEFARSLGM
E. coli 182 VYFAAGFVHEAKLH-GAHTVELNLEPSQVGNEFAEKYYGFASQVVPEFVEKLLK
S. enterica serovar Typhimurium LT2 182 VYFAAGFVHEAKLH-GAHTVELNLEPSQVGSEFEEKHYGFASQVVPEFVDKFLK
B. longum subsp. infantis 196 VYFAASIVPVAACAG-VPITIMNMGHTQYDHLASRLIH----EDIAAALPKLVD
S. cerevisiae 476 VAPVSEIVNMVPSH--VPQVLINRDP-VKHAEFDLSLLG----YCDDIAAMVAQ
Homo sapiens SIRT3 324 VEPFASLTEAVRSS--VPRLLINRDL-VGPLAWHPRSRD--VAQLGDVVHGVES
Homo sapiens SIRT1 445 VRPVALIPSSIPHE--VPQILINREP-LPHLHFDVELLG----DCDVIINELCH

Fig. 1 Deduced amino acid sequences of *L. paracasei* sirtuin aligned with sirtuin of other organisms

Single-headed arrows indicate conserved active center histidines. Double-headed arrows indicate NAD^+-binding domains (Rossmann fold). For the two counterpart proteins of *L. rhamnosus*, they are labeled as SirA* or SirB* to indicate its equivalence with LpSirA and LpSirB.

Accession numbers:

L. paracasei NRIC 0644 GenBank nucleotide ID, AB728561; *L. paracasei* NRIC 1917 GenBank nucleotide ID, AB728562; *L. paracasei* NRIC 1981 GenBank nucleotide ID, AB728563 and AB728564 (LpSirA and LpSirB, respectively); *L. paracasei* BL23 NCBI Gene ID, 6407162; *L. rhamnosus* GG NCBI Gene ID, 8424228 and 8421081 (LpSirA homolog and LpSirB homolog, respectively); *Bacillus subtilis* 168 NCBI Gene ID, 936271; *Escherichia coli* K12 NCBI Gene ID, 945687; *Salmonella* Typhimurium LT2 NCBI Gene ID, 1252739; *Bifidobacterium longum* subsp. *infantis* ATCC 15697 NCBI Gene ID, 7054471; *Saccharomyces cerevisiae* ATCC 204508 NCBI Gene ID, 851520; *Homo sapiens* NCBI Gene ID, 23411.

CHAPTER 2
Enzyme kinetics of the recombinant LpSirA protein

1. INTRODUCTION

The sirtuins were shown to catalyze a reaction that couples lysine deacetylation to the formation of nicotinamide and O-acetyl-ADP-ribose from NAD^+ and the acetylated substrate (Tanner et al., 2000; Tanny et al., 2000). Sirtuins are inhibited by nicotinamide, a product of the deacetylation reaction (Bitterman et al., 2002; Avalos et al., 2005). The human has seven sirtuins which were designated SIRT1-SIRT7. SIRT1 was shown to exert a regulatory effect on p53 by deacetylation of lysine-382. SIRT1 inhibits the p53-dependent apoptotic response by deacetylating the lysine-382 of p53 and SIRT1 reverses in part the damage-induced activation of p53. Therefore, SIRT1 in concert with other deacetylases reduces the likelihood of subsequent apoptosis, and at the same time, makes it possible for cells to return to the previous physiological state maintaining healthy balance (Vaziri et al., 2001). In parallel, many SIRT1 activators have been shown to be useful for treatment of several diseases such as diabetes, metabolic diseases, neurodegenerative diseases, cancer, and cardiovascular disease (Villalba et al., 2012; Guarente et al., 2011). In addition, screening for activators of SIRT1 enzyme activity yielded in a number of small molecule activators, all of which were plant polyphenols. Some of these Sirtuin Activating Compounds (STACs) were shown to extend yeast lifespan in a way that mimicked caloric restriction (Howitz et al., 2003). Resveratrol, one of the STACs, activated SIRT1 enzyme activity, and was expected for the treatment of age-related diseases such as type 2 diabetes (Milne et al., 2007). On the other hand, many

SIRT1 inhibitors have been shown to be useful for treatment of several diseases such as metastasis of certain cancer cells, immunodeficiency virus infections and Fragile X mental retardation syndrome (Villalba et al., 2012). For example, nicotinamide, splitomicin, sirtinol and suramin, among others were known to be sirtuin inhibitors.

In this chapter, the author made recombinant LpSirA and LpSirB by conducting with *E. coli* expression system and purified on a Nickel-affinity column. In addition, the author performed kinetics study of LpSirA using *Flour de Lys*® fluorimetric activity measurement kit.

2. MATERIALS AND METHODS

2.1 Expression and purification of the recombinant LpSirA and LpSirB.

The cloned individual DNA fragments in the pT7 Blue plasmids were further amplified using cloning primers containing artificially added restriction enzyme cutting sites for subsequent sub-cloning. Underlines in the cloning primer sequences indicate artificially added restriction enzyme recognition sites for subsequent sub-cloning (Table 1 in the chapter 1). The resulting DNA was sub-cloned into bacterial protein expression vector pET-15b (Novagen Merck Millipore, Darmstadt, Germany) at the cloning site between *Bpu*1102 I and *Xho* I. The proteins were expressed in *E. coli* BL21 (DE3) strain (Novagen Merck Millipore, Darmstadt, Germany). The DNA sequence was confirmed as described in the material and methods (p. 8). The recombinant LpSirA and LpSirB with histidine tag was generated and purified as follows:

E. coli BL21 (DE3) strain was incubated in 50 ml of L broth medium supplemented with 100 µg/ml ampicillin. The cells were grown at 37°C for 12 hours and

were inoculated to 400 ml of L broth medium. The cells were grown at 30°C to optical density (OD): 0.7 (OD: 600 nm), and then induced with 1 mM isopropyl-β-D-thiogalactoside (IPTG) at 30°C for 3 hours. Cells were harvested by centrifugation and suspended in a phosphate buffer (50 mM NaH_2PO_4, pH 8.0, 300 mM NaCl). The cells were subsequently disrupted using an ultrasonic disintegrator (Sonifier 450, Branson Ultrasonics, Emerson, Japan), and the cell debris were removed by centrifugation at 12,000 rpm for 10 min at 4°C. The recombinant protein was purified on a Nickel-affinity column (15 mm x 10 mm ϕ, bed volume 1.0 ml) (Profinity IMAC Ni-charged resin, Bio-Rad laboratories Headquarters CA, USA). After the flow through fraction was discarded, the column was washed with 10 ml of wash buffer 1 (50 mM NaH_2PO_4, pH 8.0, 300 mM NaCl, 2 mM imidazole) and 6 ml of wash buffer 2 (50 mM NaH_2PO_4, pH 8.0, 300 mM NaCl, 20 mM imidazole), and the bound proteins were eluted using 10 ml of elution buffer (50 mM NaH_2PO_4, pH 8.0, 300 mM NaCl, and 250 mM imidazole). The fractions were analyzed by SDS-polyacrylamide gel electrophoresis (SDS-PAGE). Next, the fractions were dialyzed using Sir2 buffer (20 mM HEPES-KOH, pH 7.5, 50 mM NaCl, 1 mM dithiothreitol, 1 mM EDTA). For long term storage, the dialyzed fractions were stored in Sir2 buffer supplemented with 50% glycerol at -20˚C. The protein concentration was measured by Bio-Rad protein assay system (Bio-Rad Laboratories, CA, USA). The recombinant LpSirB was produced as described above, however, the protein was found in the inclusion body of *E. coli* BL21 (DE3). Therefore, for the purification, the recombinant protein was dissolved in the presence of 8 M urea and subsequently purified as above in the presence of 8 M urea. Urea was removed during dialysis using Sir2 buffer.

2.2 Enzymatic kinetics

Kinetics studies were performed using *Flour de Lys*® fluorimetric activity measurement kit (Biomol/ENZO, Exeter, UK) according to the manufacturer's instruction. The substrate used was an acetylated peptide comprising amino acids 379-382 of human p53. The control recombinant SIRT1 protein was provided in the same kit. The reaction followed Michaelis Menten kinetics, displaying Km (constant) and Vmax (maximum reaction velocity) of SIRT1 and LpSirA on the acetylated substrate. The apparent Km and Vmax of SIRT1 and LpSirA from NRIC 0644, 1917 and 1981 were calculated from Lineweaver Burk plot obtained in the presence of 3 mM NAD^+ (fixed) and 0.2 µg of SIRT1 and LpSirA proteins from NRIC 0644, 1917 and 1981 in the reaction mixtures. The relative fluorescence unit was measured using NanoDrop 3300 Fluorospectrometer (Thermo Fisher Scientific, Waltham, MA, USA) and the conversion of the relative fluorescence unit to molar unit for substrate acetylated peptide was calculated from the standard curve using deacetylated fluorescent peptide substrate (*Flour de Lys*® deacetylated standard) provided in the kit. In addition, the author tested SIRT1 activator resveratrol and SIRT1 inhibitor suramin (Trapp et al., 2007). The optimal temperature for the enzymatic reaction was tested in the presence of 150 µM NAD^+ and 0.2 µg of SIRT1 and LpSirA proteins from NRIC 0644, 1917 and 1981 in the reaction mixtures. The tested temperatures were 15, 25, 37, 50 and 60°C. The reaction in the presence of 100 µM resveratrol followed Michaelis Menten kinetics, displaying Km (constant) and Vmax (maximum reaction velocity) of SIRT1 and NRIC 0644 LpSirA on the acetylated substrate. The apparent Km and Vmax of SIRT1 and LpSirA from NRIC 0644 were calculated from Lineweaver Burk plot obtained in the presence of 3 mM NAD^+ and another concentration enzyme protein (0.2 µg of SIRT1 and 1.5 µg of LpSirA) in the

reaction mixtures. The inhibition rate by the suramin was presented from half maximal (50%) inhibitory concentration. The apparent Vmax of SIRT1 and LpSirA from NRIC 0644 were calculated from Lineweaver Burk plot obtained in the presence of 3 mM NAD^+, 100 μM the acetylated substrate and 0.2 μg of enzyme protein in the reaction mixtures. The tested suramin concentration were 0, 125, 250, 500 and 1000 μM in the reaction mixture of LpSirA and 0, 12.5, 25, 50 and 100 μM in the reaction mixture of SIRT1.

3. RESULTS AND DISCUSSION

3.1 Expression and purification of recombinant LpSirA and LpSirB

The cDNAs of *sirA* and *sirB* were introduced in the bacterial expression system using *E. coli* BL21 (DE3), and the His-tagged recombinant proteins were affinity-purified. As shown in Fig. 1, recombinant protein preparations appeared homogeneous after SDS-PAGE and coomassie brilliant blue staining (Coomassie® Brilliant blue R 250, Merck Millipore, Darmstadt, Germany), displaying apparent molecular sizes of 29 kDa for LpSirA and 34 kDa for LpSirB products.

3.2 Enzyme kinetics of the recombinant LpSirA proteins from *L. paracasei* strains

Comparative studies were performed to examine deacetylase enzymatic activity of LpSirA proteins derived from three strains of *L. paracasei* and human SIRT1 protein. Kinetic parameters were measured to obtain Km and Vmax values as described in the method. The apparent Km values in terms of acetylated peptide substrate were determined to be 130.2 μM, 186.3 μM, 180.1 μM and 130.1 μM for human SIRT1, *L. paracasei* NRIC 0644 LpSirA, NRIC 1917 LpSirA and NRIC 1981 LpSirA, respectively (Fig. 2).

The Vmax values were initially calculated from the measurement of the relative fluorescence unit, then converted to molar unit according to the standard curve made by deacetylated fluorescent peptide provided in the *Flour de Lys*® fluorimetric activity measurement kit. The Vmax values were 257.5 nmol/min/mg, 160 nmol/min/mg, 170 nmol/min/mg and 212.5 nmol/min/mg for SIRT1, NRIC 0644 LpSirA, NRIC 1917 LpSirA and NRIC 1981 LpSirA proteins, respectively. These Km and Vmax values were calculated from Lineweaver Burk plot which was obtained in Michaelis Menten kinetics studies. Michaelis Menten kinetics was measured by average values tested three times using NRIC 0644 LpSirA, NRIC 1917 LpSirA and NRIC 1981 LpSirA proteins. Whereas, Michaelis Menten kinetics of SIRT1 protein was measured just once, because SIRT1 has been shown to deacetylate the lysine-382 of p53. The enzyme characteristics of the *L. paracasei* sirtuin proteins were comparable to human SIRT1 (Fig. 2). As for the optimal temperature for the enzymatic reaction, LpSirA proteins displayed higher optimal temperature (45-50˚C) than SIRT1 (37˚C) (Fig. 3). As for LpSirB, enzymatic activity was not measured, as this protein turned out to be precipitated again after dialysis following affinity column purification. In addition, resveratrol resulted in the decrease of the apparent km values of human SIRT1 from 93.9 μM to 60.7 μM (the average of three experiments). On the other hand, the effect of resveratrol on LpSirA was not clear as shown in Fig. 4A right panel. The reproducibility of the effect of resveratrol is still needed to be examined for NRIC 0644 LpSirA (Fig. 4A). The author thought that the effect of resveratrol on LpSirA was not clear. One of the reasons for this observation could be due to the fact that the resveratrol binding site (glu 230) of N-terminal domain as reported in human SIRT1 (Cao et al., 2015; Hubbard et al., 2013) is not existing in LpSirA. Therefore, the author thought that it is important to search for new activator which strongly activate

the enzyme activity of LpSirA. In addition, suramin inhibited deacetylase activity of both human SIRT1 (IC_{50}: 18 μM) and NRIC0644 LpSirA (IC_{50}: 359 μM) (Fig. 4B). These values were determined by average values in three times tests. The results suggest the similarity and the difference of enzyme property between human SIRT1 and LpSirA.

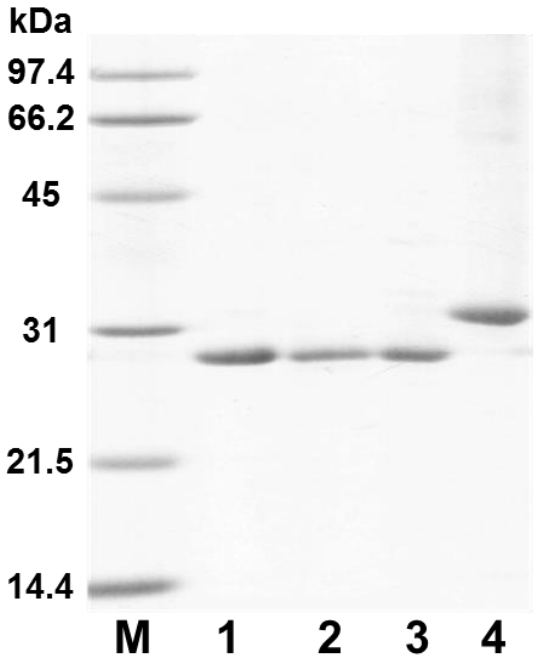

Fig. 1 SDS-PAGE analysis of Recombinant LpSirA and LpSirB

The affinity purified the His-tagged LpSirA and LpSirB proteins were separated on SDS gel and stained with Coomassie Brilliant Blue. M: Molecular weight marker (Bio-Rad LMW). Lanes 1: *L. paracasei* NRIC 0644 LpSirA, 2: *L. paracasei* NRIC 1917 LpSirA, 3: *L. paracasei* NRIC 1981 LpSirA, and 4: *L. paracasei* NRIC 1981 LpSirB. The recombinant LpSirB was found in the inclusion body of *E. coli* BL21 (DE3). Therefore, for the purification, the protein was dissolved in the presence of 8 M urea and subsequently purified as above in the presence of 8 M urea.

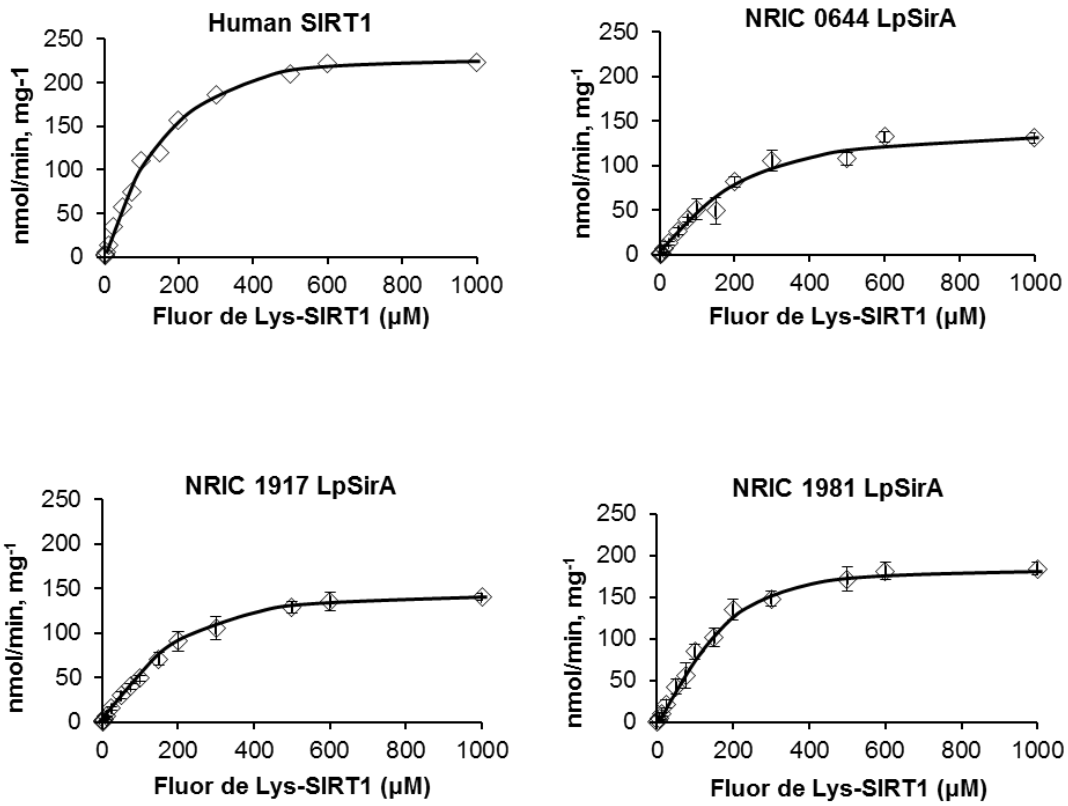

Fig. 2 Enzyme kinetics of the recombinant LpSirA proteins and SIRT1

Recombinant proteins were expressed in *E. coli* and purified on an affinity column using Nickel-loaded resin. LpSirA proteins of NRIC 0644, NRIC 1917 and NRIC 1981 showed deacetylase activities comparable to human SIRT1. The Vmax values were 257.5 nmol/min/mg, 160 nmol/min/mg, 170 nmol/min/mg and 212.5 nmol/min/mg for SIRT1, NRIC 0644 LpSirA, NRIC 1917 LpSirA and NRIC 1981 LpSirA proteins, respectively. The apparent Km values in terms of acetylated peptide substrate were determined to be 130.2 μM, 186.3 μM, 180.1 μM and 130.1 μM for human SIRT1, *L. paracasei* NRIC 0644 LpSirA, NRIC 1917 LpSirA and NRIC 1981 LpSirA, respectively. These Km and Vmax values were calculated from Lineweaver Burk plot which was obtained in Michaelis Menten kinetics studies. Error bars represent standard deviation Michaelis Menten kinetics was determined by average values of three experiments using NRIC 0644 LpSirA, NRIC 1917 LpSirA and NRIC 1981 LpSirA proteins (n=3). Whereas, Michaelis Menten kinetics of SIRT1 protein was measured just once (n=1).

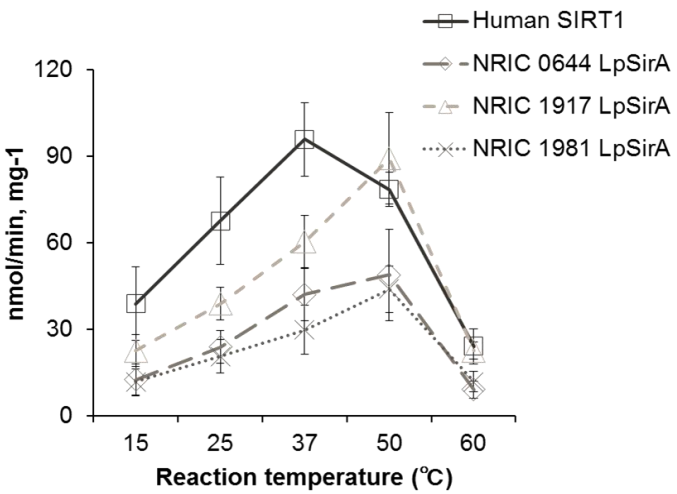

Fig. 3 The optimal temperature for the enzymatic reaction

The quadrangle indicates the human SIRT1, the rhombus indicates the NRIC 0644 LpSirA, the triangle indicates the NRIC 1917 LpSirA and the x-mark indicates the NRIC 1981 LpSirA. The optimal temperature for the enzymatic reaction was tested in the presence of 150 μM NAD^+ and 0.2 μg of each enzyme protein in the reaction mixtures. The tested temperature were 15, 25, 37, 50 and 60°C. As for the optimal temperature for the enzymatic reaction, LpSirA proteins displayed higher optimal temperature (45-50˚C) than SIRT1 (37˚C). Error bars represent standard deviation. These values were determined by average values of three experiments (n=3).

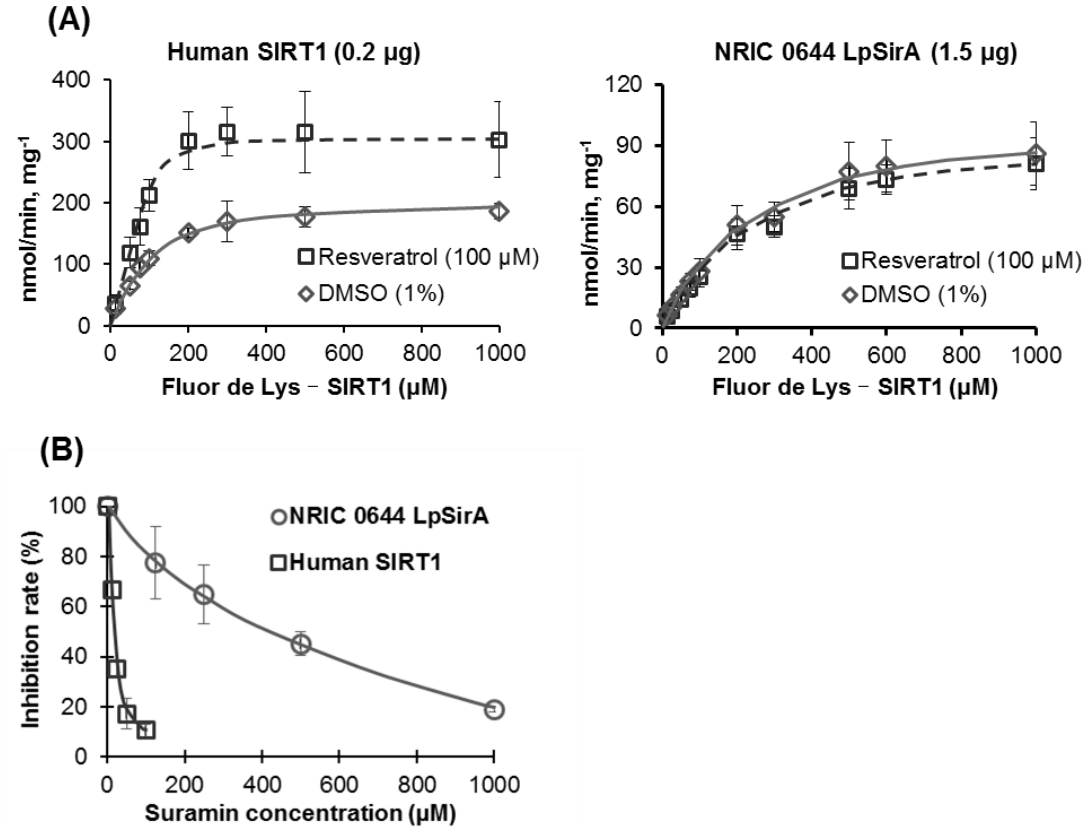

Fig. 4 Effect of resveratrol and suramin on the enzyme kinetics of reconbinant SIRT1 and LpSirA proteins

(A) Effect of resveratrol. The reaction followed Michaelis Menten kinetics, displaying Km (constant) and Vmax (maximum reaction velocity) of SIRT1 and NRIC 0644 LpSirA on the acetylated substrate. The apparent Km and Vmax of SIRT1 and LpSirA were calculated from Lineweaver Burk plot obtained in the presence of 3 mM NAD^+ with two different concentrations of enzyme protein (0.2 μg of SIRT1 and 1.5 μg of LpSirA) in the reaction mixtures. Resveratrol resulted in the decrease of the apparent km values of human SIRT1 from 93.9 μM to 60.7 μM (the average of three experiments). On the other hand, the effect of resveratrol on LpSirA was not clear as shown in Fig. 4A right panel. The reproducibility of the effect of resveratrol is still needed to be examined for NRIC 0644 LpSirA (B) The inhibition rate by the suramin was presented from half maximal (50%) inhibitory concentration (IC_{50}). The apparent Vmax of SIRT1 and LpSirA from NRIC 0644 were calculated from Lineweaver Burk plot obtained in the presence of 3 mM NAD^+, 100 μM the acetylated substrate and 0.2 μg of enzyme protein in the reaction mixtures. The tested suramin concentration were 0, 125, 250, 500 and 1000 μM in the reaction mixture of LpSirA and 0, 12.5, 25, 50 and 100 μM in the reaction mixture of SIRT1. Suramin inhibited sirtuin enzyme activities of LpSirA and SIRT1. In addition, the

IC_{50} values were 18 μM and 359 μM for SIRT1, NRIC 0644 LpSirA proteins, respectively. Error bars represent standard deviation. These values were measured by average values from three experiments (n=3).

CHAPTER 3
Identification of the sirtuin-target acetylated proteins in *L. paracasei* BL23

1. INTRODUCTION

Protein acetylation is a common process of post translational modification in both eukaryotes and prokaryotes, and it is regarded to play important roles in many biological processes (Zhao et al., 2010). Protein acetylation is reversible, dynamic, and highly conserved. The many acetylated proteins and acetylation sites have been identified in bacteria, such as the model organism *E. coli*. For example, 349 acetylated proteins were identified in *E. coli* by using nano-LC/MS/MS analysis (Zhang et al., 2013). In addition, 899 acetylated proteins were recently identified in *E. coli* (Baeza et al., 2014). This report developed and employed a novel method for directly quantifying stoichiometry of site-specific acetylation in the entire proteome of *E. coli*. Loss of *cobB* affected site specific and global acetylation stoichiometry. The acetylated proteins include many functionally important proteins, such as acetyl-coenzyme A synthetase (ACS) and chemotaxis response regulator protein (CheY). In *E. coli*, it has been shown to deacetylate ACS, thereby activating the enzyme (Starai et al., 2002). In *E. coli* the chemotactic gene *cheY* product was reported to be deacetylated by CobB protein (Li et al., 2010). Others reported an extensive global analysis using *cobB* deletion mutant of *E. coli*, and found 51 acetylated proteins in the bacterium. These proteins were sensitive to CobB and they were involved primarily in translation, central metabolism and DNA-centered processes (AbouElfetouh et al., 2015). The importance of protein acetylation as a posttranslational modification has been documented as reviewed by others (Bernal et al., 2014). On the other hand, the acetylated protein was not yet reported in LAB.

In this chapter, the author identified several candidate target proteins both *in vivo* and *in vitro* by using the recombinant LpSirA protein and sirtuin inhibitor nicotinamide (NAM), and tried to purify the candidate proteins in the cell extracts by using ammonium sulfate precipitation (0-80%), Butyl-Toyopearl column and DE52 column.

2. MATERIALS AND METHODS

2.1 Screening of the target acetylated proteins and amino acid sequencing

Hereafter, instead of the three strains, a widely studied standard strain, *L. paracasei* BL23 was used (Maze et al., 2010). The putative target proteins of sirtuin in *L. paracasei* BL23 were first screened by inhibiting sirtuin deacetylase using NAM in the culture medium. Following two successive pre-culture to ensure logarithmic growth, BL23 was cultured in MRS medium supplemented with 0, 5, 10 or 50 mM NAM for 12 hours and collected by centrifugation at 6,000 rpm. The cells were washed once with buffer A (50 mM Tris-HCl, pH 7.6, supplemented with 50 mM NaCl) and re-suspended in buffer A supplemented with 1 mM dithiothreitol and 0.1 mM PMSF. The cell extracts were then made using bead crasher (TAITEC Corp., Saitama, Japan) with glass beads (0.1 mm in diameter). In parallel, a cell extract (from cells cultured in MRS supplemented with 50 mM NAM) containing 100 μg protein was treated *in vitro* with 10 μg purified recombinant LpSirA in the presence of 10 mM NAD^+ to maximize NAD^+-dependent deacetylation. The protein concentration was measured by Bio-Rad protein assay system (Bio-Rad Laboratories, CA, USA).

2.2 Western blot analysis

From each of the *in vivo* and *in vitro* target samples obtained above, 100 μg cellular proteins were subjected to 12.5% SDS-PAGE, and blotted onto PVDF cellulose membranes (Amersham Hybond-P, GE Healthcare Buckinghamshire, UK) for 60 min at 40 V using an electroblotter (Semi-dry type NA-1512, Nihon Eido, Co. Ltd. Tokyo, Japan). Western blotting was done using anti-LpSirA primary antibody (made from the purified LpSirA, Japan Lamb co. Ltd, Hiroshima, Japan) or Acetylated-Lysine primary antibody (Cell Signaling Technology, Inc. Danvers, MA, USA) and donkey anti-rabbit IgG secondary antibody (GE Healthcare UK Ltd. Buckinghamshire, England). For the detection, an enhanced chemiluminescence (ECL) system (Pierce, USA) was used with Amersham™ ECL™ Prime Western Blotting Detection Reagent (GE Healthcare UK Ltd. Buckinghamshire, England) and Light-Capture II (AE-6981, ATTO, Tokyo, Japan).

2.3 Purification of target protein from *L. paracasei* BL23 and western blot analysis

Cells of *L. paracasei* BL23 strain were cultured in MRS medium supplemented with 50 mM NAM for 12 hours and collected by centrifugation at 6,000 rpm. The cells were washed once using the above-mentioned buffer A, and re-suspended in buffer A supplemented with 1 mM dithiothreitol and 0.1 mM PMSF. The cell extracts were then made using ultrasonic disintegrator. To purify the candidate proteins in the cell extracts, most of the proteins were first collected by ammonium sulfate precipitation (0-80%), then dialyzed (Cellulose tube 8/32, EIDIA, Tokyo, Japan), and then supplemented again with ammonium sulfate to 25% saturation. The solution was then subjected to a Butyl-Toyopearl column (Tosoh, Tokyo, Japan). Proteins were eluted by step-wise decreases in ammonium sulfate concentration and were subjected to SDS-PAGE followed by western

blotting to identify the acetylated protein. The fraction eluted with 10% ammonium sulfate containing the targets was then subjected to a DE52 column (6 mm x 15 mm ϕ, bed volume 1 ml), and the proteins were eluted by step-wise increase in NaCl concentration. The elution at 0.5 M NaCl showed single band of an acetylated 28 kDa protein. The acetylation and deacetylation by LpSirA were confirmed by Western blotting using anti-acetyl lysine antibody as described above. The fraction containing 28 kDa protein was further concentrated by acetone precipitation (80%). The precipitated protein was resolved in buffer A, and was subjected to SDS-PAGE followed by electro-blotting onto FluoroTrans® PVDF Transfer Membranes (Pall Life Sciences 600 South Wagner Road Ann Arbor, MI 48103-9019 USA). The area of the membrane containing the protein was cut out and its N-terminal amino acid sequences were determined by the Edman degradation method with a peptide sequencer PPSQ30 (SHIMAZU CORPORATION, Kyoto, Japan).

3. RESULTS AND DISCUSSION

3.1 Identification of the sirtuin-target acetylated proteins in *L. paracasei*

In an attempt to search for the endogenous substrate acetylated proteins of sirtuin in *L. paracasei*, the cells were treated with a sirtuin inhibitor, NAM, supplemented in the culture medium. After cell disruption by ultrasonic treatment, the cell extracts were subjected to SDS-PAGE followed by electro-blotting to a cellulose membrane. The results indicated that the acetylation levels of the 28 kDa protein (pointed with a filled triangle) were significantly elevated with increasing concentration of NAM supplemented in the medium (indicated at the bottom of Fig. 1A). On the other hand, when *in vitro*

deacetylation was performed with purified LpSirA protein in the presence of NAD^+ for the cell extracts prepared after culturing *L. paracasei* cells in the presence of 50 mM NAM, about 6 acetylated proteins with the molecular weights of 27, 28, 29, 31, 40 and 48 kDa showed decrease in signal intensity on western blots (Fig. 1B, indicated by small arrows for 27, 29, 31, 40 and 48 kDa proteins, and a filled triangle for 28 kDa protein). Such decrease was not observed in the absence of recombinant LpSirA, or when endogenous LpSirA contained in the extract was inhibited in the presence of NAM. Among these deacetylated proteins, the 28 kDa protein was most deacetylated *in vitro* by LpSirA and its acetylation level was increased *in vivo* with NAM. Taken together, the 28 kDa band was identified as the endogenous target sirtuin substrate, which was then subjected to purification. Proteins in the cell extracts were partially purified by ammonium sulfate precipitation, and further purified with two-step column chromatographies using Butyl sepharose and DEAE sepharose. The results showed that the purified acetylated 28 kDa protein (Fig.2 A-4 and B-4) was deacetylated by supplemented LpSirA as shown in Fig. 2C (compare lanes 1 vs. 2). The N-terminal Amino acid sequence of the 28 kDa target protein was determined by Edman degradation method to be SRYTGPRWKQ, which was perfectly identical to be that of the 30S ribosomal protein S4 of *L. paracasei* in the data bank. The function of 30S ribosomal protein S4 was first indicated for mRNA binding as a translational repressor (Tang and Draper, 1990). More recently, it was postulated to function in multiple stages of ribosome assembly by interacting with 16S rRNA (Mayerle et al., 2013). The crystal structure of 30S ribosomal protein S4 was revealed to suggest its function as RNA-binding through positively charged domain (Davies et al., 1998). It is somehow in line with this report that deacetylation of 30S ribosomal protein S4 may weaken the RNA-binding to render either

alleviation of translational repression or efficiency of ribosome assembly, which may slow down growth rate, possibly in response to environmental stresses. Also in line with this, it is noteworthy that ribosomal large subunit component MRP10 was found to be the target of eukaryotic mitochondrial sirtuin (SIRT3) in human, and it was shown to decrease protein synthesis rate using mouse model system, possibly functioning in survival under starving condition (Yang et al., 2010). The acetylation of 30S ribosomal protein S5 in bacteria has been reported, but there has been no report on the acetylation of 30S ribosomal protein S4 to our knowledge, therefore this is the first evidence that 30S ribosomal protein S4 is acetylated and can be deacetylated by LpSirA at least in *Lactobacilli*. Thus, the author presumed that LpSirA is involved in protein synthesis in *L. paracasei*, and thought that it could be able to control the protein synthesis by regulating the activity of the sirtuin. If LpSirA can control the protein expression of stress response and adhesin, the author expects that LAB may serve as better probiotics to contribute for the promotion of human health. A part of these results are on the way to be published (Atarashi et al., 2016. in press)

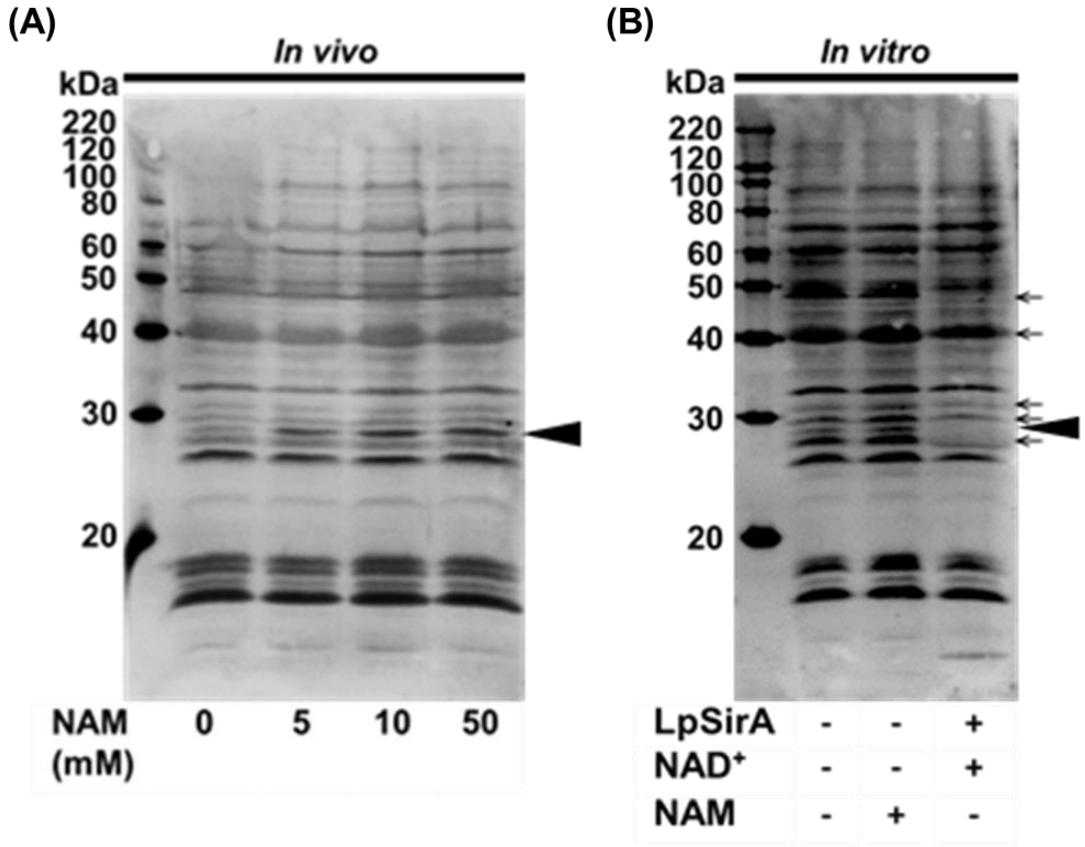

Fig. 1 Target protein substrate identification of sirtuin-mediated deacetylation
(A) *In vivo* inhibition of sirtuin using increasing concentration of NAM in the culture medium. *L. paracasei* BL23 cells were cultured in the presence of indicated concentration of NAM in the medium. In each lane, cell extract containing 100 μg protein was loaded and Western blotting was done using anti-acetylated lysine antibody. The filled triangle indicates the 28 kDa protein. (B) *In vitro* deacetylation of the target proteins by purified LpSirA supplemented with NAD^+. Cells were cultured in the medium containing 50 mM NAM. Then the cell extracts were prepared by bead crasher and were dialyzed to remove NAM. The cell extracts containing 100 μg protein were treated with materials indicated in the bottom. Concentration of NAM or NAD^+ was 10 mM each. Ten μg of purified recombinant LpSirA was supplemented in the far-right sample. Each sample was incubated at 37˚C for 1hour. The filled triangles indicate the position of the 28 kDa protein, and the small arrows indicate the proteins of 27, 29, 31, 40 and 48 kDa, whose acetylation levels were decreased by treatment with LpSirA and NAD^+.

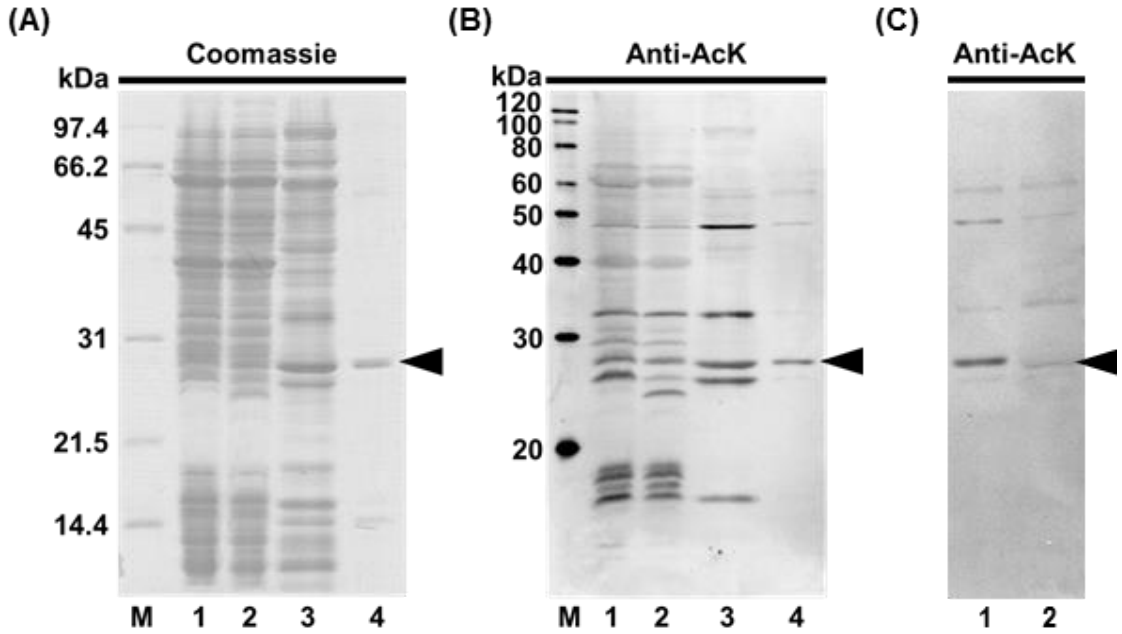

Fig. 2 Purification of the target protein from *L. paracasei* BL23

Coomassie brilliant blue staining (A) and Western blot with anti-acetylated lysine antibody (B). Lanes 1: Crude extract (100 μg protein), 2: Ammonium sulfate precipitate (100 μg protein), 3: Fraction after Butyl Toyopearl column (50 μg protein), and 4: Fraction after DEAE-cellulose column (1 μg protein). (C): *In vitro* deacetylation of the purified 28 kDa protein by LpSirA. Lanes 1: Purified 28 kDa protein (0.6 μg without treatment), and 2: Purified 28 kDa protein (0.6 μg the 28 kDa protein was incubated with 5 μg of LpSirA in the presence of 10 mM NAD^+ for 1 hour at 37˚C). The filled triangles indicate the position of the 28 kDa protein.

CHAPTER 4
Intracellular localization of sirtuin protein in *L. paracasei* BL23

1. INTRODUCTION

Sirtuin family (SIRT1-7) were demonstrated to be localized in different subcellular compartments for each family member, with SIRT6 and SIRT7 being nuclear proteins, SIRT3, SIRT4 and SIRT5 mitochondrial proteins, and SIRT1 and SIRT2 being found both in the nucleus and the cytoplasm. On the other hand, the localization of bacterial sirtuin have not yet been reported, and have not been reported under what conditions the localization can be changed. It is important to localize it appropriately in terms of the protein function. For example, it was reported that Sir2 activity is required to maintain its localization, even in resting cells, although delocalization does not occur immediately upon Sir2 inhibition (Bitterman et al., 2002). Thus, the author thought that the cellular localization could be the key to understand the function of sirtuin.

In this chapter, the author analyzed intracellular localization of LpSirA in *L. paracasei* by using immunofluorescent staining and LpSirA-Venus fusion protein, and tried to deduce deduced the function of sirtuin from its localization.

2. MATERIALS AND METHODS

2.1 Immunofluorescent staining,

LpSirA was labeled with Alexa Fluor® 488 dye (Thermo Fisher Scientific, Waltham, MA, USA) and nucleoid was stained by Hoechst 33342, Trihydrochloride,

Trihydrate (Thermo Fisher Scientific, Waltham, MA, USA). Cells of *L. paracasei* BL23 strain were cultured in MRS medium for 8 hours at 37˚C. The newly inoculated culture in MRS medium was incubated for 16 hours at 37˚C and collected by centrifugation at 6,000 rpm. Cells were suspended in PBS (phosphate buffered saline, pH 7.4, 137 mM NaCl, 2.7 mM KCl, 10 mM Na_2HPO_4, 1.8 mM $KHPO_4$). Cells were fixed onto cover glasses and treated with 4% paraformaldehyde for 20 min. Cells were washed twice with PBS and treated with methanol for 5 min at -20˚C. Cells were washed once with PBS and treated with TE buffer containing 20 mg/ml lysozyme and 1.2% (w/v) TritonX-100. Cells were washed twice with PBS containing 0.1% (w/v) Tween 20 and blocked in PBS containing 2% (w/v) BSA, 0.3% (w/v) TritonX-100 and 0.1% (w/v) NaN_3 for 10 min. Cells were probed with a rabbit anti-LpSirA antibody (1:250 dilution) in PBS containing 2% (w/v) BSA, 0.3% (w/v) TritonX-100 and 0.1% (w/v) NaN_3 for 1h at 37˚C. Following four washes with PBS containing 0.1% (w/v) Tween 20, Cells were incubated with the anti-rabbit Alexa Fluor® 488 dye antibody (1:2,000 dilution) for 1h at 37˚C and washed again four times in PBS containing 0.1% (w/v) Tween 20. Cells were stained with 5 μg/ml hoechst 33342 for 10 min and washed once with PBS containing 0.1% (w/v) Tween 20. Finally, a drop of SlowFade® Diamond (Thermo Fisher Scientific, Waltham, MA, USA) was applied to the sample, and the localization of LpSirA in *L. paracasei* BL23 was monitored by confocal microscopy.

2.2 Construction of expression vector of Venus protein in *L. paracasei* BL23

The plasmid pCS2 Venus was provided from Hiroyuki Miyoshi and Atsushi Miyawaki (RIKEN, Saitama, Japan). The full length Venus gene (720 bp) sequence was amplified by PCR using genomic DNA as template with two primers (GACAT-*Sph* I-SD-

venus-N and CGC-*BamH* I-venus-C, Table 1). The PCR was carried out using a TaKaRa PCR Thermal Cycler Dice® mini TP-100 (TAKARA BIO INC, Shiga, Japan) and PrimeSTAR® Max DNA Polymerase (TAKARA BIO INC, Shiga, Japan) with the following conditions: 20 cycles of denaturation (98°C, 10 sec), annealing (60°C, 15 sec) and extension (72°C, 3 min). The PCR product encoding Venus was cloned into bacterial protein expression vector pLPM11 at the cloning site between *Sph* I and *BamH* I. The pLPM11 plasmid vector was provided from Dr. Akinobu Kajikawa (Department of Applied Biology and Chemistry, Tokyo University of Agriculture, Tokyo, Japan), and the protein expression was induced by galactose. The pLPM11 plasmid was transformed into *E. coli* DH5α cells (Nippon Gene Co., Ltd, Tokyo, Japan). The transformed cells were selected on LB plates containing 100 μg/ml ampicillin. Plasmid DNAs were isolated from *E. coli* cells using Genopure Plasmid Maxi Kit (Roche Basel, Schweiz) according to the manufacturer's instruction. The pLPM11 construct (2 μg) was transformed into competent *L. paracasei* BL23 cells by electroporation using Gene Pulser II (Bio-Rad laboratories Headquarters CA, USA).

2.3 Preparation of competent *L. paracasei* BL23 cells

L. paracasei BL23 cells inoculated in 3 ml of MRS medium, and the cells were grown for 16 hours at 37˚C. One ml of the culture was inoculated to 50 ml of pre-warmed (37˚C) MRS medium, and the cells were grown at 37˚C in water bath until OD: 660 reached 0.6. The cells were collected by centrifugation at 2,500 rpm for 10 min at 4˚C. The supernatant was discarded carefully, and the cells were washed once gently with 30 ml of ice-cold 1 mM sterilized HEPES buffer. Next, the cells were washed twice gently with 1 ml of ice-cold HEPES buffer and the cells were washed once gently with 1 ml of

ice-cold HEPES buffer containing 0.3 M sucrose (HEPES-sucrose). The pelleted cells were resuspended gently in 0.5 ml of ice-cold HEPES-sucrose and were aliquoted into 100 µl and plated in sterilized 200 µl PCR tubes. Finally, the tubes were frozen with liquid N_2 and the tube were stored at -80˚C.

2.4 Construction of expression vector of LpSirA-Venus fusion protein and its introduction to *L. paracasei* BL23

The strain of *L. paracasei* NRIC 0644 was cultured in MRS broth at 37˚C overnight. Genomic DNA was extracted from the cultures as described in DNeasy Blood & Tissue Kit (QIAGEN, Venlo, Netherlands) according to the manufacturer's instruction. The full length LpSirA gene sequence (693 bp) was amplified by PCR using genomic DNA as template with the two primers (CCTA-*BamH* I-*sirA*-N and GAT-*BamH* I-*sirA*-C, Table 1). The PCR was carried out using a TaKaRa PCR Thermal Cycler Dice® mini TP-100 (TAKARA BIO INC, Shiga, Japan) and PrimeSTAR® Max DNA Polymerase (TAKARA BIO INC, Shiga, Japan) with the following conditions: 20 cycles of denaturation (98°C, 10 sec), annealing (60°C, 15 sec) and extension (72°C, 3 min). The PCR product was treated with Alkaline Phosphatase (TAKARA BIO INC, Shiga, Japan) for 30 min at 50˚C. The dephosphorylated PCR product encoding LpSirA was cloned into pCS2 Venus plasmid which harbors previously incorporated Venus at the cloning site BamHI. The *sirA*-Venus fusion gene was amplified by PCR using genomic DNA as template with the two primers (GACAT-*Sph* I-SD-*sirA*-N and CGC-*Bst*P I-venus-C, Table 1). The PCR was carried out using a TaKaRa PCR Thermal Cycler Dice® mini TP-100 (TAKARA BIO INC, Shiga, Japan) and PrimeSTAR® Max DNA Polymerase (TAKARA BIO INC, Shiga, Japan) with the following conditions: 20 cycles of

denaturation (98°C, 10 sec), annealing (60°C, 15 sec) and extension (72°C, 3 min).The PCR product encoding *sirA*-venus fusion gene was cloned into the bacterial protein expression vector pLPM11 at the cloning site between *Sph* I and *Bst*P I. DNA sequence of the *sirA*-venus fusion gene was confirmed by analyzing dye-labeled extension products using BigDye® terminator v3.1 cycle sequencing kit (Applied Biosystems, Carlsbad, CA) subjected to a DNA sequencer 3100 Avant Genetic Analyzer. The sequence data were determined following sequencing both directions of the DNAs. Sequencing and cloning primers are listed in the Table 1. The pLPM11 plasmid was transformed into *E. coli* DH5α cells (Nippon Gene Co., Ltd, Tokyo, Japan). The transformed cells were selected on L agar plates containing 100 μg/ml ampicillin. Plasmid DNAs were isolated from *E. coli* cell cultures using a Genopure Plasmid Maxi Kit (Roche Basel, Schweiz) according to the manufacturer's instruction. The pLPM11 construct (5 μg) was transformed into competent *L. paracasei* BL23 cells by electroporation using Gene Pulser II (Bio-Rad laboratories Headquarters CA, USA).

2.5 Fluorescence imaging of LpSirA-Venus fusion protein in *L. paracasei* BL23

The LpSirA-Venus highly expressing strain was inoculated into a 5 ml MRS medium containing 5 μg/ml erythromycin and the cells were grown for 12 hours at 37°C. The 5 ml culture was washed with 0.86 % saline and inoculated into a 5 ml of GYP medium containing 1% (w/v) galactose, 1% (w/v) yeast extract, 0.5% (w/v) peptone, 0.2% (w/v) beef extract, 0.2 % (w/v) sodium acetate trihydrate, 0.5% (w/w) salt solution, 0.05 % (w/w) Tween 80 (where the glucose was replaced with galactose). The LpSirA-Venus protein was induced for 16 hours at 37°C by 1% (w/v) galactose in GYP medium (where the glucose was replaced with galactose). Finally, the cells of LpSirA-Venus high

expresser were fixed on a slide glasses which was covered with GYP-agar (where the glucose was replaced with galactose), and incubated for 2 hours at 37°C. The localization of LpSirA in the LpSirA-Venus high expresser strain was examined by confocal microscopy.

3. RESULTS AND DISCUSSION

3.1 Intracellular localization of LpSirA in *L. paracasei*

The author analyzed intracellular localization of LpSirA in fixed *L. paracasei* BL23 cells by using immunofluorescent staining. In late logarithmic phase cells, the result showed that LpSirA was localized on the division plates and cellular poles during cell division (Fig. 1). Next, the author analyzed intracellular localization of LpSirA in the living cells by using LpSirA-Venus fusion protein in *L. paracasei* BL23. The result indicated that LpSirA-Venus protein was localized along a spiral in the cytoplasm (Fig. 2).

In *Bacillus subtilis,* RacA and the cell division protein DivIVA were reported as a protein which is localized in the cellular poles. RacA protein promotes the movement to the cellular poles of the nucleoid, and the cell division protein DivIVA connects the RacA to cellular poles. RacA acts as a bridge between the replication origin region and the cellular poles, and assembles into an adhesive patch at a centromere-like element near the replication origin, causing chromosomes to stick at the poles (Ben-Yehuda et al., 2003). FtsZ and FtsA proteins were reported to be the proteins which are localized to the division plates during cell division in *B. subtilis.* FtsA is a cytosolic division protein that interacts directly with FtsZ. The bacterial tubulin homolog FtsZ was reported to assemble

into a ring-like structure. FtsA ensures recruitment of the membrane-bound division proteins by ensuring correct formation of the Z ring (Jensen et al., 2005). Further, MreB protein and the MinD proteins were localized as a spiral in the cytoplasm. The bacterial actin homolog MreB forms large fibrous spirals under the cell membrane of rod-shaped cells, where they are involved in cell-shape determination (Ent et al., 2001). MinD localizes as a spiral in *B. subtilis* cell (Barak et al., 2008). MinC localizes MinD to the cellular poles where it prevents FtsZ assembly until the cell size doubles (ready, that is for division). DivIVA and MinD recruit MinC to division sites, rather than mediating the stable polar localization previously thought to restrict MinC activity to the pole. Together, *B. subtilis* MinC does not inhibit FtsZ assembly at the cellular poles, but rather prevents polar FtsZ rings adjacent to new cellular poles from supporting cell division (Gregory et al., 2014). In an analogy to these findings in studies using *B. subtilis,* these mechanisms were illustrated in Fig. 3. The intracellular localization of LpSirA by using immunofluorescent staining showed that LpSirA localized on the division plates and at the cellular poles during cell division. In addition, the intracellular localization of LpSirA in living cells by using LpSirA-Venus fusion protein showed that LpSirA localized as a spiral in the cytoplasm. Those localization pattern of LpSirA closely resemble to the intracellular localization of MinC and MinD. Thus, the author presumed that LpSirA is involved in cell division in *L. paracasei*.

Table 1. PCR primers used in cloning and sequencing

Primer	5' to 3'	Restriction enzyme	Recognition sequence
venus-N	ATGGTGAGCAAGGGCGAGGAG		
venus-C	TTACTTGTACAGCTCGTCCAT		
CCTA-*Bam*H I-*sirA*-N	CCTAGGATCCATGTTTGATCTGCAAACTGC	*Bam*H I	GGATCC
GATC-*Bam*H I-*sirA*-C (Stop codon is not existing)	GATCGGATCCGACTACCAGCTTCGCAAATACG	*Bam*H I	GGATCC
CGC-*Bam*H I-venus-C	CGCGGATCCTTACTTGTACAGCTCGTCCATGCC	*Bam*H I	GGATCC
GACAT-*Sph* I-SD-*sirA*-N	GACATGCATGCTGATGAAAGGAGGGACCATAT ATGTTTGATCTGCAAACTGCA	*Sph* I	GCATGC
GACAT-*Sph* I-SD-venus- N	GACATGCATGCTGATGAAAGGAGGGACCATAT ATGGTGAGCAAGGGCGAGGAG	*Sph* I	GCATGC
CGC-*Bst*P I-venus-C	CGCGGTNACCTTACTTGTACAGCTCGTCCATGCC	*Bst*P I	GGTNACC
venus-200	ACGGCCTGCAGTGCTTCGCCC		
venus-220	GGGCGAAGCACTGCAGGCCGT		
venus-520	CCTCGATGTTGTGGCGGATCT		

Underlines indicate artificially added sequences corresponding to the recognition sites of the restriction enzymes listed herein

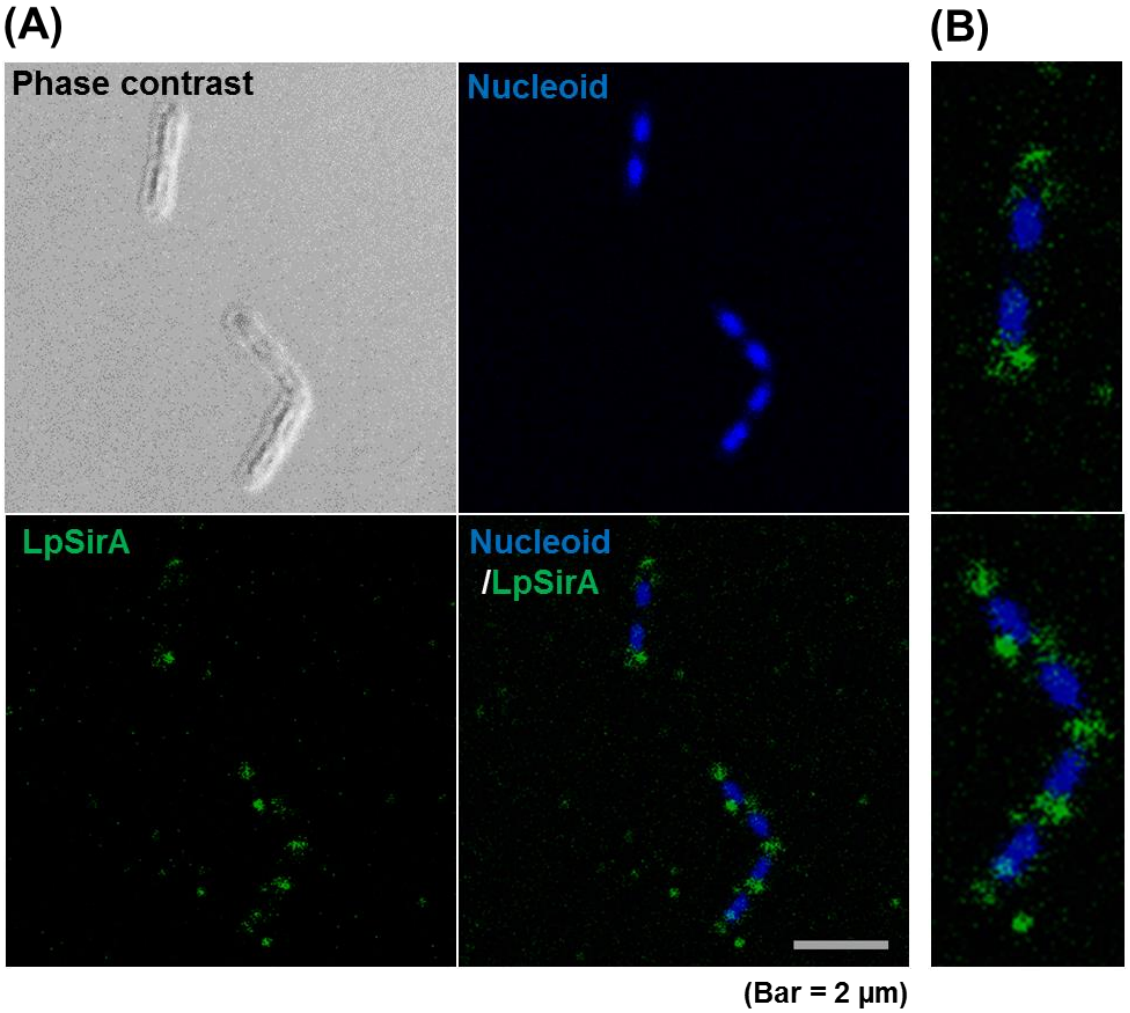

Fig. 1 Intracellular localization of LpSirA by using immunofluorescent staining
(A) The LpSirA protein was labeled with Alexa Fluor® 488 dye (Green) and nucleoid was stained by Hoechst 33342 (Blue). The cells of *L. paracasei* BL23 were incubated for 16 hours at 37˚C (late logarithmic growth phase). Cells were fixed on cover glasses and treated with 4% paraformaldehyde for 20 min. Cells were probed with a rabbit anti-LpSirA antibody (1:250 dilution) and anti-rabbit Alexa Fluor® 488 dye antibody (1:2,000 dilution) for 1h at 37˚C. The nucleoid of the cells were stained with 5 μg/ml hoechst 33342 for 10 min. Finally, a drop of SlowFade® Diamond was applied to the sample and localization of LpSirA was examined in *L. paracasei* BL23 by confocal microscopy. The result showed that LpSirA was localized on the division plates and cellular pole during cell division. Scale bar indicates 2 μm. (B) The image was obtained by enlarging the image of merge (Nucleoid/LpSirA).

(A)

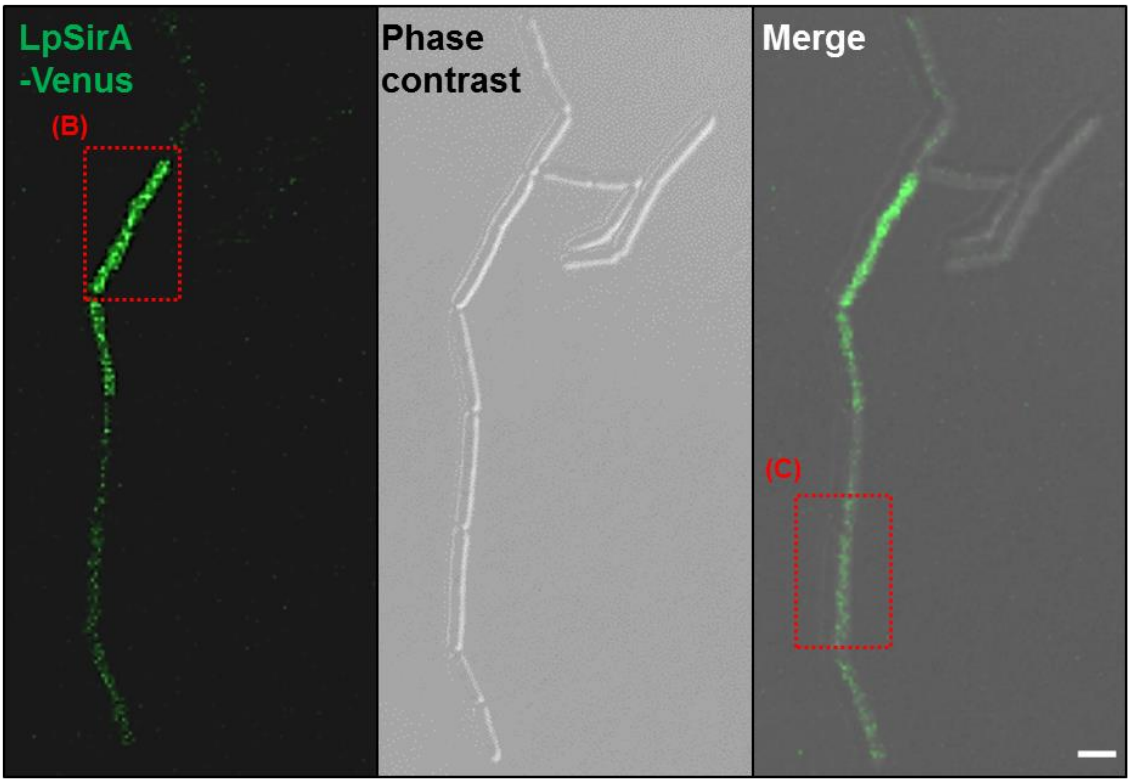

(Bar = 2 μm)

(B)

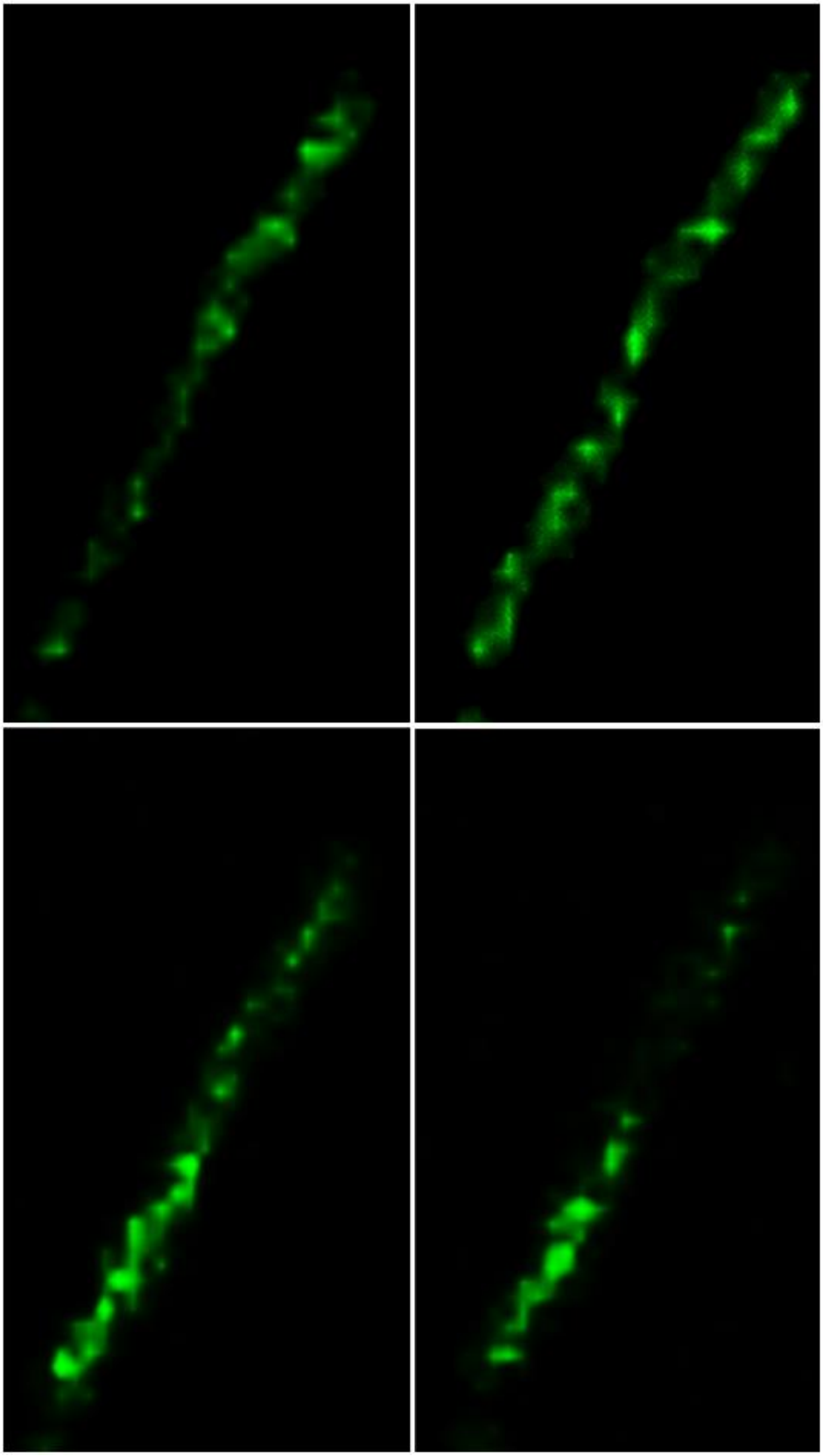

(C)

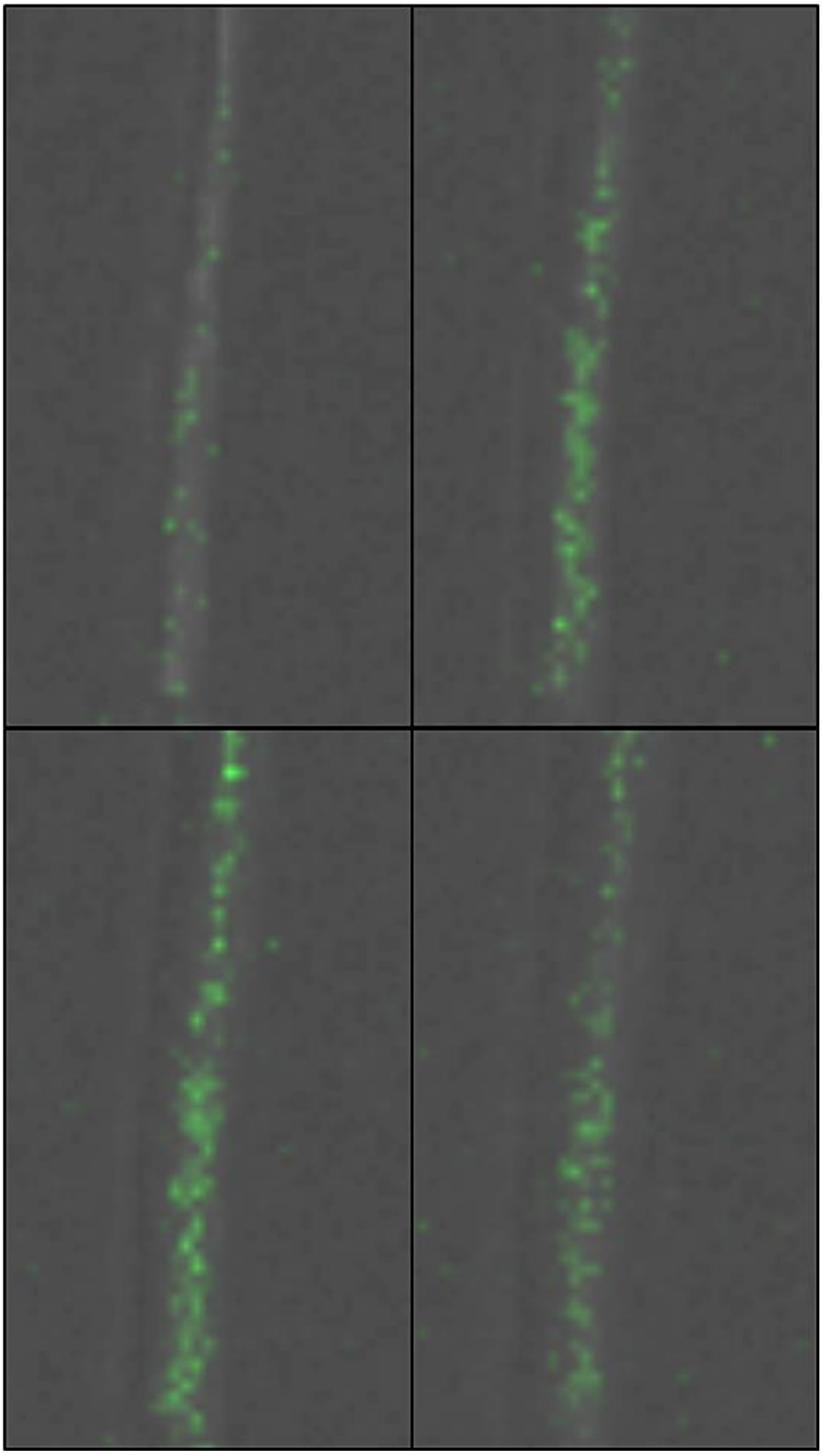

Fig. 2 Intracellular localization of LpSirA by using LpSirA-Venus fusion protein
(A) The intracellular localization of sirtuin using LpSirA-Venus fusion protein (green) in the living cells of *L. paracasei* BL23. The LpSirA-Venus protein was induced for 16 hours at 37°C by GYP medium (where the glucose was replaced with galactose). The Cells of LpSirA-venus were fixed on slide glasses which was covered with GYP-agar (where the glucose was replaced with galactose), and incubated for 2 hours at 37°C. The localization of LpSirA was examined by confocal microscopy. Scale bar indicates 2 μm. (B) Magnified image of the red square in the far left panel (LpSirA-Venus) of Fig. 2A. LpSirA-Venus signals in four different focal planes are shown. (C) Magnified image of the red square in the far right panel (merge) of Fig. 2A. LpSirA-Venus signals in four different focal planes are shown. The results indicated that LpSirA-Venus protein was localized as a spiral in the cytoplasm.

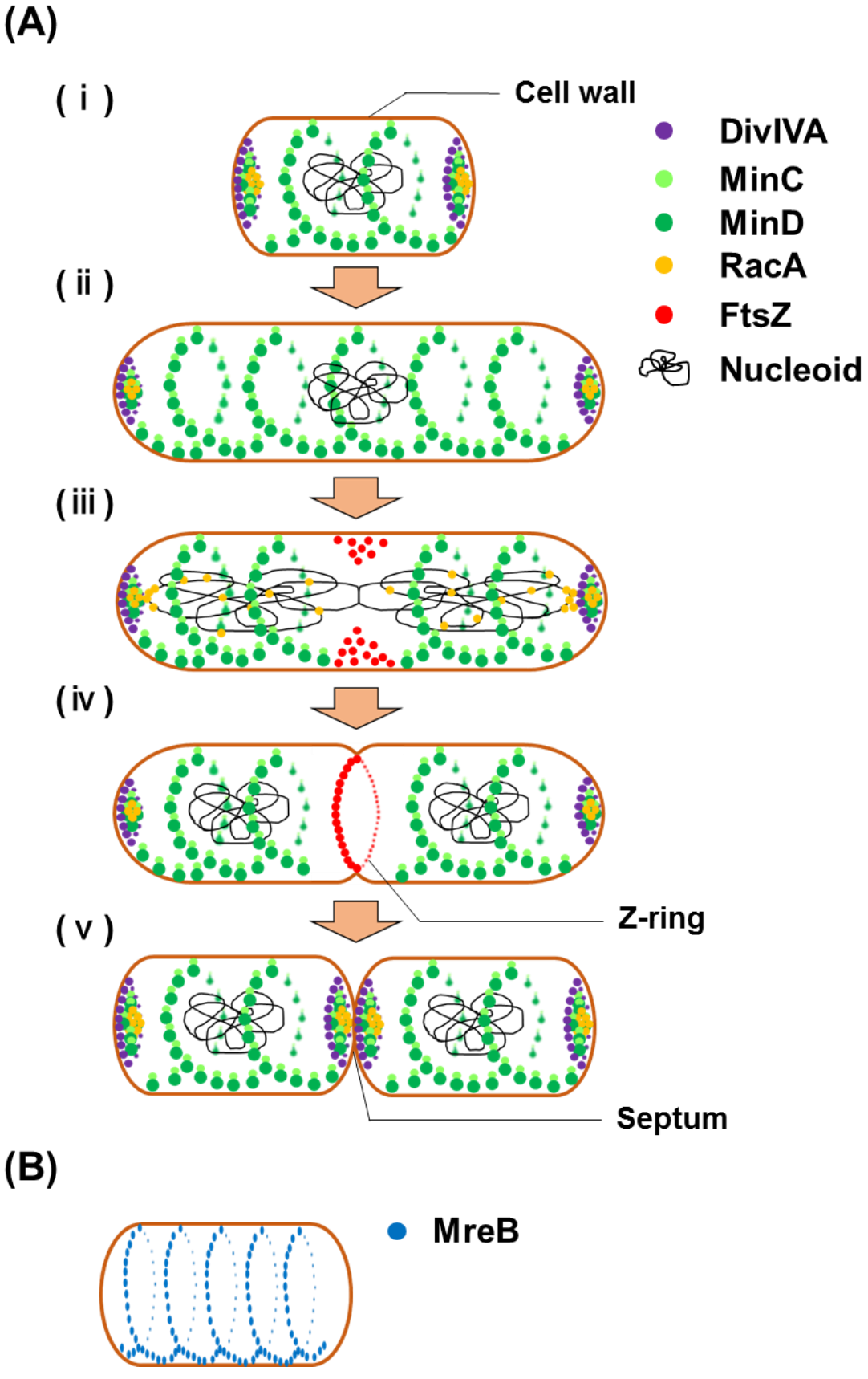
(A)
(i)
Cell wall
DivIVA
MinC
MinD
RacA
FtsZ
Nucleoid
(ii)
(iii)
(iv)
Z-ring
(v)
Septum
(B)
MreB

Fig. 3 The intracellular localization of cytoskeleton protein and cell division protein in *Bacillus subtilis*

(A) The intracellular localization of cell division protein during cell division. (ⅰ) DivIVA (violet) and RacA (orange) localize at cellular poles. MinC (light green) and MinD (green) localizes as a spiral in the cytoplasm, and it also localizes at the cellular poles. DivIVA recruits RacA to the cellular poles. (ⅱ) MinC and MinD inhibits FtsZ (red) assembly in order to inhibit cell division during the cell elongation phase to avoid premature division. (ⅲ) The nucleoids (black) are separated to opposite cellular poles by RacA, after completion of the cell elongation. While, MinC and MinD moves away from the center of the cell, and FtsZ starts to assemble. (ⅳ) The assembly of FtsZ forms as a ring in the center of the cell and forms into the Z-ring. (ⅴ) The Z-ring makes septum and cell division starts. After completion of cell division, MinC and MinD localizes as a spiral in the cytoplasm to restart cell elongation. (B) The intracellular localization of MreB. MreB (blue), the cell shape-determining bacterial actin homolog, localizes as a spiral in the cytoplasm.

These illustration were made in reference to a variety of articles (Ben-Yehuda et al., 2003; Jensen et al., 2005; Ent et al., 2001; Barak et al., 2008; Gregory et al., 2014) describing cell division mechanism in *B. subtilis*.

The intracellular localization of LpSirA by using immunofluorescent staining showed that LpSirA localized on the division plates and at the cellular poles during cell division. In addition, the intracellular localization of LpSirA in living cells by using LpSirA-Venus fusion protein showed that LpSirA localized as a spiral in the cytoplasm. Those localization pattern of LpSirA closely resemble to the intracellular localization of MinC and MinD. Thus, the author presumed that LpSirA is involved in cell division in *L. paracasei*.

REFERENCES

AbouElfetouh A, Kuhn ML, Hu LI, Scholle MD, Sorensen DJ, Sahu AK, Becher D, Antelmann H, Mrksich M, Anderson WF, Gibson BW, Schilling B, Wolfe AJ. (2015) The *E. coli* sirtuin CobB shows no preference for enzymatic and nonenzymatic lysine acetylation substrate sites. *Microbiology open.* **4**, 66-83.

Atarashi H, Kawasaki S, Niimura Y, Tanaka N, Okada S, Shiwa Y, Endo A and Nakagawa J. (2016) Identification of Sirtuin and its target as the ribosomal protein S4 in *Lactobacillus paracasei*. *J Gen Appl Microbiol*. in press.

Anderson RM1, Bitterman KJ, Wood JG, Medvedik O, Sinclair DA. (2003) Nicotinamide and PNC1 govern lifespan extension by calorie restriction in Saccharomyces cerevisiae. *Nature.* **423**, 181-185.

Avalos JL, Celic I, Muhammad S, Cosgrove MS, Boeke JD, Wolberger C. (2002) Structure of a Sir2 enzyme bound to an acetylated p53 peptide. *Mol. Cell.* **10**, 523-535.

Baeza J, Dowell JA, Smallegan MJ, Fan J, Amador-Noguez D, Khan Z, Denu JM. (2014) Stoichiometry of site-specific lysine acetylation in an entire proteome. *J Biol Chem*. **289**, 21326-21338.

Barák I, Muchová K, Wilkinson AJ, O'Toole PJ, Pavlendová N. (2008) Lipid spirals in *Bacillus subtilis* and their role in cell division. *Mol Microbiol*. **68**, 1315-1327.

Ben-Yehuda S, Rudner DZ, Losick R. (2003) RacA, a bacterial protein that anchors chromosomes to the cell poles. *Science*. **299**, 532-536.

Bernal V, Castaño-Cerezo S, Gallego-Jara J, Écija-Conesa A, de Diego T, Iborra JL, Cánovas M. (2014) Regulation of bacterial physiology by lysine acetylation of proteins. *N. Biotechnol*. **31**, 586-595.

Blagosklonny, MV. (2010) Linking calorie restriction to longevity through sirtuins and autophagy: any role for TOR, *Cell Death Dis*. **1**, e12.

Bitterman KJ, Anderson RM, Cohen HY, Latorre-Esteves M, Sinclair DA. (2002) Inhibition of silencing and accelerated aging by nicotinamide, a putative negative regulator of yeast sir2 and human SIRT1. *J Biol Chem*. **277**, 45099-45107.

Cao D, Wang M, Qiu X, Liu D, Jiang H, Yang N, Xu RM. (2015) Structural basis for allosteric, substrate-dependent stimulation of SIRT1 activity by resveratrol. *Genes Dev*. **29**, 1316-25.

Clemente JC, Ursell LK, Parfrey LW, Knight R. (2012) The impact of the gut microbiota on human health: an integrative view. *Cell*. **148**, 1258-70.

Cleveland J, Montville TJ, Nes IF, Chikindas ML. (2001) Bacteriocins: safe, natural antimicrobials for food preservation. *Int J Food Microbiol*. **71**, 1-20.

Cohen HY, Miller C, Bitterman KJ, Wall NR, Hekking B, Kessler B, Howitz KT, Gorospe M, de Cabo R, Sinclair DA. (2004) Calorie restriction promotes mammalian cell survival by inducing the SIRT1 deacetylase. *Science*. **305**, 390-392.

Davies C, Gerstner RB, Draper DE, Ramakrishnan V, White SW. (1998) The crystal structure of ribosomal protein S4 reveals a two-domain molecule with an extensive RNA-binding surface: one domain shows structural homology to the ETS DNA-binding motif. *Embo j*. **17**, 4545-4558.

De Ruijter AJ, van Gennip AH, Caron HN, Kemp S, van Kuilenburg AB. (2003) Histone deacetylases (HDACs): characterization of the classical HDAC family. *Biochem J*. **370**, 737-749.

FAO/WHO Working Group. (2002) Guidelines for the Evaluation of Probiotics in Food. Joint FAO/WHO Working Group Report on Drafting Guidelines for the Evaluation of Probiotics in Food

Fritze CE, Verschueren K, Strich R, Easton Esposito R. (1997) Direct evidence for SIR2 modulation of chromatin structure in yeast rDNA. *Embo j*. **16**, 6495-6509.

Frye, RA. (2000) Phylogenetic classification of prokaryotic and eukaryotic Sir2-like proteins. *Biochem. Biophys. Res. Commun*. **273**, 793-798.

Gardner JG, Escalante-Semerena JC. (2009) In *Bacillus subtilis*, the sirtuin protein

deacetylase, encoded by the *srtN* gene (formerly *yhdZ*), and functions encoded by the acuABC genes control the activity of acetyl coenzyme A synthetase. *J. Bacteriol*. **191**, 1749-1755.

Gardner JG, Grundy FJ, Henkin TM, Escalante-Semerena JC. (2006) Control of acetyl-coenzyme A synthetase (AcsA) activity by acetylation/deacetylation without NAD^+ involvement in *Bacillus subtilis*. *J. Bacteriol*. 188, 5460-5468.

Goldin BR, Gorbach SL. (2008) Clinical indications for probiotics: an overview. *Clin Infect Dis*. **46.** S96-100, S144-51.

Gray SG, Ekström TJ. (2001) The human histone deacetylase family. *Exp Cell Res*. **262**, 75-83.

Gregory JA, Becker EC, Pogliano K. (2014) *Bacillus subtilis* MinC destabilizes FtsZ-rings at new cell poles and contributes to the timing of cell division. *Genes Dev*. **22**, 3475-3488.

Guarente L. Kenyon C. (2000) Genetic pathways that regulate ageing in model organisms. *Nature*. **408**, 255-262.

Guarente L. (2011) Sirtuins, Aging, and Medicine. *N Engl J Med*. **364**, 2235-2244.

Hirschey MD, Shimazu T, Capra JA, Pollard KS, Verdin E. (2011) SIRT1 and SIRT3

deacetylate homologous substrates: AceCS1, 2 and HMGCS1, 2. *Aging*. **3**, 635-642.

Howitz KT, Bitterman KJ, Cohen HY, Lamming DW, Lavu S, Wood JG, Zipkin RE, Chung P, Kisielewski A, Zhang LL, Scherer B, Sinclair DA. (2003) Small molecule activators of sirtuins extend *Saccharomyces cerevisiae* lifespan. *Nature*. **425**, 191-196.

Hubbard BP, Gomes AP, Dai H, Li J, Case AW, Considine T, Riera TV, Lee JE, E SY, Lamming DW, Pentelute BL, Schuman ER, Stevens LA, Ling AJ, Armour SM, Michan S, Zhao H, Jiang Y, Sweitzer SM, Blum CA, Disch JS, Ng PY, Howitz KT, Rolo AP, Hamuro Y, Moss J, Perni RB, Ellis JL, Vlasuk GP, Sinclair DA. (2013) Evidence for a common mechanism of SIRT1 regulation by allosteric activators. *Science*. **339**, 1216-9.

Imai S, Armstrong CM, Kaeberlein M, Guarente L. (2000) Transcriptional silencing and longevity protein Sir2 is an NAD-dependent histone deacetylase. *Nature*. **403**, 795-800.

Isolauri E, Arvola T, Sütas Y, Moilanen E, Salminen S. (2000) Probiotics in the management of atopic eczema. *Clin Exp Allergy*. **30**, 1604-1610.

Jensen SO, Thompson LS, Harry EJ. (2005) Cell division in *Bacillus subtilis*: FtsZ and FtsA association is Z-ring independent, and FtsA is required for efficient midcell Z-Ring assembly. *J Bacteriol*. **187**, 6536-6544.

Kanfi Y, Naiman S, Amir G, Peshti V, Zinman G, Nahum L, Bar-Joseph Z, Cohen HY. (2012) The sirtuin SIRT6 regulates lifespan in male mice. *Nature*. **483**, 218-221.

Klar AJ, Fogel S, Macleod K. (1979) MAR1-a Regulator of the HMa and HMalpha Loci in *Saccharomyces cerevisiae*. *Genetics*. **93**, 37-50.

Li R, Gu J, Chen YY, Xiao CL, Wang LW, Zhang ZP, Bi LJ, Wei HP, Wang XD, Deng JY, Zhang XE. (2010) CobB regulates *Escherichia coli* chemotaxis by deacetylating the response regulator CheY. *Mol. Microbiol*. **76**, 1162-1174.

Lin SJ, Defossez PA, Guarente L. (2000) Requirement of NAD and SIR2 for life-span extension by calorie restriction in *Saccharomyces cerevisiae*. *Science*. **289**, 2126-2128.

Ma Q, Wood TK. (2011) Protein acetylation in prokaryotes increases stress resistance. *Biochem. Biophys. Res. Commun*. **410**, 846-851.

Matsuda T, Fujimura S, Suda H, Matsufuji Y, Nakagawa J. (2011) Alteration of ethanol tolerance caused by the deficiency in the genes associated with histone deacetylase complex in budding yeast. *Biosci. Biotechnol. Biochem*. **75**, 1829-1831.

Mazé A, Boël G, Zúñiga M, Bourand A, Loux V, Yebra MJ, Monedero V, Correia K, Jacques N, Beaufils S, Poncet S, Joyet P, Milohanic E, Casarégola S, Auffray Y, Pérez-Martínez G, Gibrat JF, Zagorec M, Francke C, Hartke A, Deutscher J. (2010) Complete genome sequence of the probiotic *Lactobacillus casei* strain BL23. *J Bacteriol*. **192**, 2647-2648.

Mayerle M, Woodson SA (2013) Specific contacts between protein S4 and ribosomal RNA are required at multiple stages of ribosome assembly. *RNA.* **19**, 574-585.

Milne JC, Lambert PD, Schenk S, Carney DP, Smith JJ, Gagne DJ, Jin L, Boss O, Perni RB, Vu CB, Bemis JE, Xie R, Disch JS, Ng PY, Nunes JJ, Lynch AV, Yang H, Galonek H, Israelian K, Choy W, Iffland A, Lavu S, Medvedik O, Sinclair DA, Olefsky JM, Jirousek MR, Elliott PJ, Westphal CH. (2007) Small molecule activators of SIRT1 as therapeutics for the treatment of type 2 diabetes. *Nature*. **450**, 712-716.

Saka K, Ide S, Ganley AR, Kobayashi T. (2013) Cellular senescence in yeast is regulated by rDNA noncoding transcription. *Curr Biol*. **23**, 1794-1798.

Sakamoto I, Igarashi M, Kimura K, Takagi A, Miwa T, Koga Y. (2001) Suppressive effect of *Lactobacillus gasseri* OLL 2716 (LG21) on *Helicobacter pylori* infection in humans. *J Antimicrob Chemother*. **47**, 709-710.

Sanders BD, Jackson B, Marmorstein R. (2010) Structural basis for sirtuin function: what we know and what we don't. *Biochim. Biophys. Acta*. **1804**, 1604-1616.

Shiwa Y, Atarashi H, Tanaka N, Okada S, Yoshikawa H, Endo A, Miyaji T, Nakagawa J. (2015) Genome Sequences of Three Strains of *Lactobacillus paracasei* of Different Origins and with Different Cholate Sensitivities. *Genome Announc.* **3**, e00178-15.

Starai VJ, Celic I, Cole RN, Boeke JD, Escalante-Semerena JC. (2002) Sir2-dependent

activation of acetyl-CoA synthetase by deacetylation of active lysine. *Science*. **298**, 2390-2392.

Tang CK, Draper DE. (1990) Evidence for allosteric coupling between the ribosome and repressor binding sites of a translationally regulated mRNA. *Biochemistry.* **29**, 4434-4439.

Tanner KG, Landry J, Sternglanz R, Denu JM. (2000) Silent information regulator 2 family of NAD- dependent histone/protein deacetylases generates a unique product, 1-O-acetyl-ADP-ribose. *Proc Natl Acad Sci.* **19**, 14178-14182.

Tanny JC, Moazed D. (2001) Coupling of histone deacetylation to NAD breakdown by the yeast silencing protein Sir2: Evidence for acetyl transfer from substrate to an NAD breakdown product. *Proc Natl Acad Sci.* **98**, 415-420.

Thao S, Chen CS, Zhu H, Escalante-Semerena JC. (2010) Nepsilon-lysine acetylation of a bacterial transcription factor inhibits Its DNA-binding activity. *PLoS One* **5**, e15123.

Trapp J, Meier R, Hongwiset D, Kassack MU, Sippl W, Jung M. (2007) Structure-activity studies on suramin analogues as inhibitors of NAD^+-dependent histone deacetylases (sirtuins). *ChemMedChem*. **2**, 1419-1431.

Van den Ent F, Amos LA, Löwe J. (2001) Prokaryotic origin of the actin cytoskeleton. *Nature*. **413**, 39-44.

Vaziri H, Dessain SK, Ng Eaton E, Imai SI, Frye RA, Pandita TK, Guarente L, Weinberg RA. (2001) *hSIR2*^{SIRT1} functions as an NAD-dependent p53 deacetylase. *Cell*. **19**, 149-159.

Villalba JM, Alcaín FJ. (2012) Sirtuin activators and inhibitors. *Biofactors*. **38**, 349-359.

Yang Y, Cimen H, Han MJ, Shi T, Deng JH, Koc H, Palacios OM, Montier L, Bai Y, Tong Q, Koc EC. (2010) NAD^+-dependent deacetylase SIRT3 regulates mitochondrial protein synthesis by deacetylation of the ribosomal protein MRPL10. *J. Biol. Chem*. **285**, 7417-7429.

Zhao S, Xu W, Jiang W, Yu W, Lin Y, Zhang T, Yao J, Zhou L, Zeng Y, Li H, Li Y, Shi J, An W, Hancock SM, He F, Qin L, Chin J, Yang P, Chen X, Lei Q, Xiong Y, Guan KL. (2010) Regulation of cellular metabolism by protein lysine acetylation. *Science*. **327**, 1000-1004.

Zhang K, Zheng S, Yang JS, Chen Y, Cheng Z. (2013) Comprehensive profiling of protein lysine acetylation in *Escherichia coli. J Proteome Res.* **12**, 844-851.

ACKNOWLRDGEMENTS

The author wishes to express many sincere thanks to Professor Junichi Nakagawa, Tokyo university of Agriculture, for his guidance and valuable advice during the course this study.

The author wishes to express many sincere thanks to Associate Professor Akihito Endo, Tokyo university of Agriculture, for his kind advice, valuable discussion and continuous warm encouragement during the course this study.

The author wishes to express many sincere thanks to Professor Yoichi Niimura, Tokyo university of Agriculture, for determination of N-terminal amino acid sequence, his kind advice, during the course this study.

The author wishes to express many sincere thanks to Professor Shinji Kawasaki, Tokyo university of Agriculture, for determination of N-terminal amino acid sequence, his kind advice, during the course this study.

The author wishes to express many sincere thanks to Professor Sanae Okada, Tokyo university of Agriculture, for providing the three *L. paracasei* strains, his kind advice, during the course this study.

The author wishes to express many thanks to Dr. Yuh Shiwa for determination of draft genome sequence of the three *L. paracasei* strains during the course of this study.

The author wishes to express many thanks to Professor Hirofumi Yoshikawa for determination of draft genome sequence of the three *L. paracasei* strains during the course of this study.

The author wishes to express many sincere thanks to Dr. Akinobu Kajikawa, Tokyo university of Agriculture, for providing the pLPM11 plasmid vector and

L. paracasei BL23 strain, his kind advice, during the course this study.

The author wishes to express many sincere thanks to Professor Naoto Tanaka, Tokyo university of Agriculture, for analysis of sirtuin genome sequence, his kind advice, during the course this study.

The author wishes to express many sincere thanks to Professor Atsushi Miyawaki, Laboratory for Cell Function Dynamics, Brain Science Institute RIKEN for providing the pCS2 Venus plasmid vector, during the course this study.

The author wishes to express many sincere thanks to Professor Hiroyuki Miyoshi, RIKEN (the institute of physical and chemical research) for providing the pCS2 Venus plasmid vector, during the course this study.

The author wishes to express many sincere thanks to Associate Professor Tatsuro Miyaji, Tokyo university of Agriculture, for his kind advice, continuous warm encouragement during the course this study.

The author wishes to express many sincere thanks to Assistant Professor Syuki Fujimura, Tokyo university of Agriculture, for her kind advice, continuous warm encouragement during the course this study.

The author wishes to express many thanks to Miss Glaezel Torres M Sc, Mr. Yuya Yoshida and Mr. Ryoji Tanaka, for analysis of sirtuin enzyme kinetics and cooperativeness during the course of this study.

The author wishes to express many thanks to Miss. Satomi Saito, Miss. Senrin Koku, Mr. Yuki Hasegawa and Miss. Marie Ishigami, for analysis of intracellular localization of LpSirA protein and cooperativeness during the course of this study.

Special thanks are due to Miss. Yoshimi Matsufuji-Baba, Mr. Keita Miyata, Mr. Takao Matsuda, Mr. Norihide Higashi, Mr. Shinichiro Miyashita, Miss. Yuko Obuchi, Mr.

Satoshi Kano, Mr. Shintaro Hayashi, Miss Noriko Eguchi, Mr. Kenichti Ozawa, Miss. Hiromi Mizuno, Miss Ayumi Sato, Mr. Takeshi Kurose, Mr. Motoaki Senba, Miss. Yuriko Ehara, Miss. Yuki Saotome, Mr. Masahiro Hattori, Miss Mayu Watanabe, Miss. Hiromi Inada, Mr. yuichiro Suzuki, Miss Misaki Masubuchi, Miss. Humie Ariyoshi, Mr. Fumiya Shimizu, Mr. Samu Ikehara, Mr. Mitsuki Kusakari, Miss. Misa Kawaguchi, Miss. Yukiko Syukunobe. Miss. Yuka Murai, Mr Takuya Gonda, Mr. Seitaro Saito and Mr. Kyosuke Konno for their friendliness and cooperativeness during this study.

Finally, I would like to acknowledge the affectionate support of my family.

ABSTRACT

Sirtuin, often referred as the longevity gene, was first identified as SIR2 in yeast and its homologous genes have been widely found in both eukaryotic and prokaryotic organisms. In addition, the main enzyme activity of sirtuin proteins were proven that it was a NAD^+-dependent deacetylase of which the substrates are histones, p53 and other acetylated proteins in the nucleus or cytoplasm. In prokaryotes, sirtuin gene was identified as *cobB*, encoding a cobalamin processing enzyme, and later its involvement in regulating metabolic enzymes, transcription factors, chemotactic proteins and others as NAD^+-dependent deacetylase. On the other hand, little is known about its roles in lactic acid bacteria (LAB).

LAB are widely consumed by human as food fermentation starters and as probiotics. Probiotics are live bacteria that are thought to be beneficial in preventing several health conditions. According to the 2002 definition by the World Health Organization (WHO), probiotics are "live microorganisms which, when administered in adequate amounts, confer a health benefit on the host." Therefore, those probiotics bacteria must be alive in probiotics product before they were administered to the host. In addition, the important function of the probiotics was known to regulate the functions of intestine and immunopotentiative actions. Therefore, the author assumed that it is important to increase stress tolerance, adhesion to intestinal tract and production of the useful substances by LAB in order to confer more beneficial health effects on the host. In this study, the author intended to analyze the role of sirtuin in LAB.

In the chapters 1 and 2, the author analyzed sirtuin homolog genes of LAB and analyzed enzyme kinetics of the recombinant *Lactobacillus paracasei* sirtuin proteins. In the chapter 3, the author identified several candidate target proteins both *in vivo* and *in*

vitro by using the recombinant LpSirA protein and sirtuin inhibitor nicotinamide (NAM). One of the target was identified as 30S ribosomal protein S4. In the chapter 4, the author analyzed intracellular localization of sirtuin using immunofluorescent staining and LpSirA-Venus fusion protein in *L. paracasei*.

Chapter 1. Identification of sirtuin genes in the genomes of the *L. paracasei* strains and its homology to sirtuins of related bacteria

The author demonstrated that almost all LAB have homologs of eukaryotic sirtuin. Interestingly, the author was not able to find the gene in *Lactococcus spp. Carnobacterium spp. and Melissococcus spp.* In a previous study, the author's group determined draft genome sequences of three *L. paracasei* strains NRIC 0644, NRIC 1917 and NRIC 1981 (Shiwa et al., 2015). The sirtuin genes of three strains identified highly homologous (99.9%) to those of *L. paracasei* BL23. The author tentatively designated the gene as *sirA* (indicating the first sirtuin homolog of *L. paracasei*). Interestingly, there was another sirtuin isozyme found in the genome of strain NRIC 1981, which was hit by BLAST for *L. rhamnosus* GG sirtuin with 78% identity. We designated this second gene as *sirB*, which was not found in the genomes of the strains NRIC 0644, and NRIC 1917. LpSirA encoded by *sirA* (693 bp) gene was shown to have two conserved active histidine residues and the NAD^+-binding motif as reported in human SIRT1. On the other hand, the LpSirB encoding by *sirB* (726 bp) gene contained similar NAD^+-binding domains, but only one conserved active histidine residue (his 79) site. When comparison was made using LALIGN program, the LpSirA sequence was 26.2% homologous to yeast Sir2 (BL23 LpSirA residues 8-226 vs *S. cerevisiae* Sir2 residues 251-518) and 29.4% homologous to human SIRT1 (BL23 LpSirA residues 3-208 vs SIRT1 residues 245-469).

The amino acid sequence homology of LpSirA proteins with sirtuins of *E. coli*, *Salmonella enterica* serovar Typhimurium LT2 and *B. subtilis* were 29.3%, 29.5% and 31.1% respectively. The amino acid sequence of LpSirB protein showed only 80% homology to other reported *L. rhamnosus* sirtuins which share 94-97 % homology with each other.

Chapter 2. Enzyme kinetics of the recombinant LpSirA protein

Expression and purification of recombinant *L. paracasei* sirtuin was conducted with *E. coli* expression system. The *sirA* and *sirB* were cloned into bacterial protein expression vector pET-15b. The constructed pET-15b plasmid was transformed into *E. coli* BL21 (DE3) to express recombinant LpSirA and LpSirB. The recombinant proteins with histidine tag were expressed and purified on a Nickel-affinity column. However, the recombinant LpSirB protein was found in the inclusion body of *E. coli* BL21 (DE3). Therefore, for the purification, the protein was dissolved in the presence of 8 M urea. Recombinant proteins were detected in single bands as apparent molecular sizes of 29 kDa for LpSirA, and 34 kDa for LpSirB on SDS-PAGE.

Kinetic studies were performed using *Flour de Lys*® fluorimetric activity measurement kit. The relative fluorescence unit was measured using NanoDrop 3300 Fluoropectrometer. The substrate used was an acetylated peptide comprising amino acids 379-382 of human p53. The control recombinant SIRT1 protein was provided in the same kit. The apparent Km and Vmax of SIRT1 and LpSirA from NRIC 0644, 1917 and 1981 were calculated from Line weaver Burk plot obtained in the presence of 3 mM NAD^+ (fixed) and 0.2 μg of each enzyme protein in the reaction mixtures. The standard curve was calculated from using deacetylated fluorescent peptide substrate (*Flour de Lys*®

deacetylated standard) provided in the kit. In addition, the author tested SIRT1 activator resveratrol and SIRT1 inhibitor suramin. The apparent Km values were determined to be 130.2 μM, 186.3 μM, 180.1 μM and 130.1 μM for human SIRT1, *L. paracasei* NRIC 0644 LpSirA, NRIC 1917 LpSirA and NRIC 1981 LpSirA, respectively. The Vmax values were 257.5 nmol/min/mg, 160 nmol/min/mg, 170 nmol/min/mg and 212.5 nmol/min/mg for SIRT1, NRIC 0644 LpSirA, NRIC 1917 LpSirA and NRIC 1981 LpSirA proteins, respectively. The optimal temperature for the enzymatic reaction of LpSirA proteins displayed higher optimal temperature (45-50˚C) than SIRT1 (37˚C). In addition, Resveratrol decreased in the apparent Km values of human SIRT1, but the conclusion has not been reached yet on the resveratrol effects to apparent Km values of NRIC 0644 LpSirA. Therefore, in addition to examine the reproducibility, the author thinks it is important to search for new activator which strongly activate the enzyme activity of LpSirA. Suramin inhibited deacetylase activity of both human SIRT1 (IC_{50}: 18 μM) and NRIC0644 LpSirA (IC_{50}: 359 μM). The results suggests the similarity and the difference of enzyme property between human SIRT1 and LpSirA.

Chapter 3. Identification of the sirtuin-target acetylated proteins in *L. paracasei* BL23.

Hereafter, instead of the three strains, a widely studied standard strain, *L. paracasei* BL23 was used. The putative target proteins of sirtuin in *L. paracasei* BL23 were first screened by inhibiting sirtuin deacetylase using NAM in the culture medium. In parallel, cell extracts (from cells cultured in MRS supplemented with 50 mM NAM) containing 100 μg protein was treated *in vitro* with 10 μg purified recombinant LpSirA in the presence of 10 mM NAD^+ to maximize NAD^+-dependent deacetylation. From each

of the *in vivo* and *in vitro* target samples obtained above, 100 μg cellular protein was subjected to 12.5% SDS-PAGE, and blotted onto PVDF cellulose membrane. Western blotting was done using anti-LpSirA primary antibody or Acetylated-Lysine primary antibody, together with donkey anti-rabbit IgG secondary antibody. The results from each of the *in vivo* and *in vitro* samples indicated that the 28 kDa acetylated protein was the target proteins of sirtuin. Furthermore, the 28 kDa acetylated protein was purified using ammonium sulfate precipitation (0-80%), Butyl-Toyopearl column and DE52 column. The elution at 0.5 M NaCl from DE52 column showed single band of an acetylated 28 kDa protein, and this protein was deacetylated by LpSirA. The fraction containing 28 kDa protein was further concentrated by acetone precipitation (80%) and subjected to SDS-PAGE followed by electro-blotting onto FluoroTrans® PVDF Transfer Membrane. Its N-terminal amino acid sequences were determined by the Edman degradation method using a peptide sequencer PPSQ30. The N-terminal Amino acid sequence of the 28 kDa target protein was determined to be SRYTGPRWKQ, which was perfectly identical to that of 30S ribosomal protein S4 of *L. paracasei* in the data bank. The function of 30S ribosomal protein S4 was known to assemble the rRNA together with 30S ribosomal subunit protein S5 and S12. Additionally, the ribosomal large subunit component MRP10 of mitochondria was deacetylated by mitochondrial sirtuin (SIRT3), and it was found to decrease protein synthesis rate. Thus, the author presumed that LpSirA is involved in the regulation of protein synthesis in *L. paracasei* BL23.

Chapter 4. Intracellular localization of sirtuin protein in *L. paracasei* BL23

First, the author analyzed intracellular localization of sirtuin using anti LpSirA antibody in *L. paracasei* BL23. Cells were fixed on cover glasses and treated with 4%

paraformaldehyde for 20 min. Cells were probed with a rabbit anti-LpSirA antibody (1:250 dilution) and anti-rabbit Alexa Fluor® 488 dye antibody (1:2,000 dilution) for 1h at 37˚C. The nucleoid of the cells were stained with 5 μg/ml hoechst 33342 for 10 min. Finally, a drop of SlowFade® Diamond was applied to the sample and localization of LpSirA was examined in *L. paracasei* BL23 by Confocal Microscopy. The result showed that LpSirA was localized on the division plates and cellular poles during cell division.

Next, the author analyzed intracellular localization of sirtuin using LpSirA-venus fusion protein in the living cells of *L. paracasei* BL23. The *sirA* gene sequence (693 bp) was cloned into pCS2 Venus plasmid equipped with an incorporated Venus gene. The *sirA*-venus fusion gene was cloned into bacterial protein expression vector pLPM11. The pLPM11 construct (5 μg) was transformed into competent *L. paracasei* BL23 cells by electroporation. Transformant cells expressing LpSirA-Venus were inoculated into 5 ml MRS medium containing erythromycin and were grown for 12 hours at 37°C in incubator. The 5 ml culture was washed with 0.86 % saline and inoculated to 5 ml of GYP medium (where the glucose was replaced galactose). Finally, the localization of LpSirA in the LpSirA-Venus high expresser strain was examined by confocal microscopy. The result indicated that LpSirA-Venus protein was localized with a regular pattern, such as a spiral in the cytoplasm. In *Bacillus subtilis,* FtsZ in the Z-ring was shown to be localized to the division plates during cell division. In the cellular pole, there are RacA protein which promotes the movement to the cell pole of the nucleoid, and the cell division protein DivIVA which is connecting the RacA to cellular poles. Further, the actin homolog MreB protein and the MinC and MinD proteins were localized as a spiral in the cytoplasm. Thus, the author presumed that LpSirA is involved in cell division in *L. paracasei* BL23.

In this thesis, the author found that the existence of sirtuin gene in LAB and their deacetylase enzyme activities in three strains of *L. paracasei*. In addition, the author revealed that the target protein of LpSirA in *L. paracasei* BL23 is 30S ribosomal protein S4 which is involved in protein synthesis. Using immunofluorescent staining, the localization of LpSirA protein was shown to be localized to the division plates and cellular poles during cell division. Additionally, using the LpSirA-Venus high expresser strain, LpSirA protein was localized with a regular pattern, such as a spiral in the cytoplasm of living LAB. In conclusion, the author concluded that the function of sirtuin may likely be involved in protein synthesis control and cell division in *L. paracasei*. Thus, the author expects that sirtuin may serve as a novel criteria to select LAB for developing better probiotics to contribute for the promotion of human health.

ABSTRACT (in Japanese)

長寿遺伝子として知られているサーチュインは、SIR2 として酵母において最初に同定され、その相同遺伝子は真核生物および原核生物で広く確認されている。加えて、サーチュインタンパク質の主な働きは細胞質や核内において、ヒストン、p53 および他のアセチル化タンパク質を基質とする NAD^+ 依存的脱アセチル化であることが報告されている。原核生物において、サーチュインは、コバラミン合成酵素をコード化する *cobB* として特定され、その後、脱アセチル化酵素として、代謝酵素、転写制御因子および走化性タンパク質に関与することが報告された。一方で、乳酸菌におけるサーチュインの役割については未だ不明である。

乳酸菌は、発酵食品のスターターおよびプロバイオティクスとして広く利用されている。2002 年、WHO によりプロバイオティクスは「一定量摂取することで、宿主に有益な作用をもたらす、生きた微生物」として定義された。この事から、プロバイオティクスは宿主が摂取するまでは生存していることが求められる。プロバイオティクスの重要な作用として腸管内細菌叢のバランスを保つことや、免疫賦活作用が挙げられる。その為、乳酸菌がより良いプロバイオティクスとして働くうえで、ストレス耐性能、腸管付着作用および乳酸菌生産物質を増加させることは宿主の健康にとって重要である。そこで、本研究では乳酸菌がより良いプロバイオティクスとしての機能を発揮する上で、サーチュインの役割について解析を行った。

本研究ではまず、乳酸菌におけるサーチュイン遺伝子の同定を行い、供試菌である *Lactobacillus paracasei* と他種サーチュインとの相同性解析を行った (第 1 章)。更に、同定した *L. paracasei* サーチュインタンパク質について組換えタンパク質を作製、精製し、脱アセチル化活性の測定を行った (第 2 章)。次に、サーチュインの脱アセチル化標的タンパク質の探索を組換えサーチュインタンパク

質とサーチュインの阻害剤であるニコチンアミドを用いて行った。そのうちの精製した標的基質タンパク質のアミノ酸配列決定を行い、30S ribosomal protein S4 であることを同定した (第 3 章)。更に、サーチュインタンパク質の局在観察を免疫蛍光染色法と蛍光タンパク質である Venus とサーチュインの融合タンパク質を用いて、解析を行った (第 4 章)。

第 1 章　*L. paracasei* におけるサーチュイン遺伝子の同定および他種サーチュインとの相同性解析

本章では乳酸菌におけるサーチュイン遺伝子の同定を行い、ほぼ全ての乳酸菌がサーチュイン遺伝子を少なくとも 1 つ保有することを明らかとした。しかし、興味深いことに、*Lactococcus* 属、*Carnobacterium* 属および *Melissococcus* 属からはサーチュイン遺伝子を確認することができなかった。著者のグループは以前に、*L. paracasei* NRIC 0644, NRIC 1917 および NRIC 1981 の 3 株の全遺伝子配列の解析を行っており (Shiwa et al., 2015)、これら 3 株より同定を行ったサーチュイン遺伝子は *L. paracasei* BL23 のサーチュイン遺伝子と 99.9% の相同性を示し、このサーチュインを *sirA* と命名した。更に、NRIC 1981 株にのみ存在し、*L. rhamnosus GG* のサーチュインと 78% の相同性を示したサーチュインは *sirB* とした。またアミノ酸配列の特徴として、*sirA* 遺伝子よりコードされる LpSirA タンパク質は 2 つの活性中心と NAD^+ 結合部位を保存しており、一方、*sirB* よりコードされる LpSirB タンパク質は NAD^+ 結合部位を保存しているが、活性中心は 1 つしか保存していなかった。加えて、LALIGN を用いて、他種サーチュインとアミノ酸配列の相同性を比較解析した所、LpSirA は酵母の Sir2 と 26.2% (BL23 LpSirA 8-226 aa に対して *S. cerevisiae* Sir2 251-518 aa) ヒトの SIRT1 とは 29.4% の相同性を示した (BL23 LpSirA 3-208 aa に対して SIRT1 245-469 aa)。更

に *Escherichia coli*、*Salmonella enterica* serovar Typhimurium LT2 および *Bacillus subtilis* とはそれぞれ 29.3%、29.5%、31.1% の相同性を示した。また LpSirB のアミノ酸配列は菌種間での相同性が 94-97% を示す *L. rhamnosus* サーチュインと 80% の相同性を示した。

第 2 章　組換え *L. paracasei* サーチュインタンパク質の酵素活性測定

大腸菌組換え系を用いて *L. paracasei* サーチュインの発現および精製を行った。*sirA* および *sirB* を pET-15b plasmid vector に挿入し、組換えタンパク質 LpSirA および LpSirB を発現させるため、*E. coli* BL21 (DE3) へ形質転換を行った。His-tag が融合した組換えタンパク質はニッケルアフィニティーカラムにより精製され、各画分は SDS-PAGE により解析を行った。しかし、LpSirB は *E. coli* BL21 (DE3) 菌体内にて不溶化した為、8 M の Urea を用いて可溶化を行った。その結果、組換えタンパク質は分子量が LpSirA で約 29 kDa、LpSirB で約 34 kDa の単一バンドとして、検出された。更にこの精製 LpSirA を用いて、アフィニティー精製ポリクローナル抗体を作成した。

酵素活性は *Flour de Lys*® fluorimetric activity measurement kit を用いて解析し. 相対蛍光強度は NanoDrop 3300 Fluorospectrometer を用いて測定を行った。ヒト p53 (379-382 aa) からなるアセチル化ペプチドを基質として用い、コントロールである組換え SIRT1 タンパク質は、同キット付属のタンパク質を用いた。NRIC 0644、NRIC 1917、NRIC 1981 株の LpSirA および SIRT1 の Km 値と Vmax 値は反応液中に 3 mM 固定濃度の NAD^+ と 0.2 μg の各酵素を添加した場合に得られる Lineweaver Burk plot から、計算を行った。検量線はキット付属の Deacetylated fluorescent peptide substrate (*Flour de Lys*® deactylated standard)を用いて、計算を行った。これに加えて、著者は SIRT1 の賦活剤であるレスベラトロールと SIRT1

の阻害剤であるスラミンの酵素活性への影響を試験した。Km 値は、SIRT1、*L. paracasei* NRIC 0644 LpSirA、NRIC 1917 LpSirA および NRIC 1981 LpSirA で、それぞれ 130.2 μM、186.3 μM、180.1 μM および 130.1 μM を示した。Vmax 値は、SIRT1、NRIC 0644 LpSirA、NRIC 1917 LpSirA および NRIC 1981 LpSirA でそれぞれ 257.5 nmol/min/mg、160 nmol/min/mg、170 nmol/min/mg および 212.5 nmol/min/mg を示した。更に、酵素の至適温度は、LpSirA で、SIRT1（37˚C）より高い至適温度を（45-50˚C）を示すことを発見した。加えて、レスベラトロールはヒト SIRT1 の Km 値を減少させることを確認したが、NRIC 0644 LpSirA の Km 値への影響に関しては未だ結論は出ていない。その為、再現性を確認すると共に、LpSirA の酵素活性を強力に賦活する、新規賦活剤の探索もこれからの重要なテーマであると考える。また、スラミンはヒト SIRT1 および NRIC 0644 LpSirA 両方の脱アセチル化酵素活性の阻害を行い、酵素活性が 50% 阻害されるスラミンの濃度はヒト SIRT1 で 18 μM および NRIC 0644 LpSirA で 359 μM であることが明らかとなった。これらの結果はヒト SIRT1 と *L. paracasei* LpSirA の酵素の諸性質の類似点と相違点を示している。

第 3 章　*L. paracasei* BL23 におけるサーチュインの標的タンパク質の探索

以後の実験に関しては *L. paracasei* 3 株の代わりに、基準株である *L. paracasei* BL23 に絞って行った。*L. paracasei* BL23 サーチュインの標的タンパク質は、まず初めに *in vivo* 試験として、培地中に阻害剤である NAM を添加し脱アセチル化酵素を阻害することにより、選抜を行った。その他にも *in vitro* 試験として、100 μg の粗抽出液 (50 mM NAM が添加された MRS で培養された細胞) に対して、NAD^+ 依存的な脱アセチル反応を最大限に行う為に、10 mM NAD^+ および 10 μg の精製組換え LpSirA を添加し、酵素反応を行った。*in vivo* および *in vitro* 試

験結果より得られたタンパク質 100 µg を、12.5% ゲルを用いた SDS-PAGE を行い、PVDF 膜へ転写を行った。Western blotting は 1 次抗体として精製 LpSirA を用いて作製した anti-LpSirA primary antibody および市販 Acetylated-Lysine primary antibody を用い、2 次抗体として donkey anti-rabbit IgG secondary antibody を用いた。*in vivo* および *in vitro* の試験結果を総合すると、サーチュインの標的タンパク質として 28 kDa のアセチル化タンパク質の存在が示された。続いて、28 kDa のアセチル化タンパク質を、硫安沈殿 (0-80%)、Butyl-Toyopearl カラムおよび DE52 カラムを用いて精製を行った。0.5 M NaCl での溶出画分において、28 kDa のアセチル化タンパク質の単一バンドを示し、このタンパク質は LpSirA によって脱アセチル化されることが確認された。28 kD のタンパク質を含む画分は、アセトン沈殿 (80%) により、さらに濃縮された後、SDS-PAGE を行い、FluoroTrans® PVDF Transfer Membrane へ転写を行った。転写後の 28 kDa タンパク質の N 末端アミノ酸配列は、Peptide sequencer PPSQ30 を用いたエドマン分解法により解析された。その結果、28 kDa の標的タンパク質の N 末端アミノ酸配列は SRYTGPRWKQ であることが示され、そのアミノ酸配列はデータバンクに登録されている *L. paracasei* の 30S ribosomal protein S4 のものと完全に一致した。30S ribosomal protein S4 の機能として、30S ribosomal protein S5 および S12 と共に、rRNA と会合を行うことが知られている。加えて、ミトコンドリアのサーチュイン (SIRT3) がミトコンドリアの ribosomal large subunit component MRP10 を脱アセチル化し、それにより、タンパク質合成量が減少したという事が知られている。それ故、著者は *L. paracasei* BL23 においてサーチュインはタンパク質合成に関与する事を推測した。

第 4 章　*L. paracasei* BL23 におけるサーチュインタンパク質の局在解析

まず初めに、著者は抗 LpSirA 抗体を用いて免疫蛍光染色法による局在観察を行った。細胞はカバーグラスに接着させ、4% のパラホルムアルデヒドで 20 分間の固定化処理を行った。細胞は Anti-LpSirA antibody (250 倍希釈) および anti-rabbit Alexa Fluor® 488 dye antibody (2,000 倍希釈) を 37˚C で 1 時間反応させることで観察を行った。細胞の核様体は 5 µg/ml の Hoechst 33342 で染色を行い、SlowFade® Diamond を細胞に滴下し、共焦点顕微鏡を用いて *L. paracasei BL23* における LpSirA の局在観察を行った。その結果、LpSirA が分裂細胞における分裂面と細胞極に局在することが観察された。次に、著者は生細胞における局在を観察する為に、LpSirA-Venus 融合タンパク質を用いた局在観察を行った。*sirA* 遺伝子 (693 bp) は venus 遺伝子を含んだ pCS2 plasmid vector へ挿入され、*sirA*-venus 融合遺伝子を、pLPM11 plasmid vector に挿入し、この pLPM11 (5 µg) を、エレクトロポーレーション法を用いて、*L. paracasei* BL23 に形質転換を行った。LpSirA-Venus 高発現株はエリスロマイシン含有の MRS 培地にて、37°C で 12 時間の前培養を行い、0.86% の生理食塩水を用いて洗浄後で、5 ml の GYP 培地 (glucose を galactose に交換) に植菌を行った。最後に、LpSirA-Venus 高発現株を GYP-agar (glucose を galactose に交換) で覆われたカバーガラスに植菌を行い、共焦点顕微鏡によって LpSirA-Venus タンパク質の局在観察を行った。その結果、LpSirA-Venus タンパク質が細胞質に螺旋のような規則性をもって局在することが観察された。枯草菌においては、分裂面に局在するタンパク質として Z リングを合成する FtsZ が存在する。細胞極には、核様体の細胞極への移動を促進させる RacA および、RacA を細胞極につなぐ細胞分裂タンパク質 DivIVA が存在する。さらに細胞質において螺旋状に局在するタンパク質として、アクチンホモログである MreB タンパク質および FtsZ の重合を阻害する MinC および MinD タンパク質が存在する。これらの事から、著者は *L. paracasei* BL23 においてサ

ーチュインは細胞分裂に関与する事を推測した。

本論文において、著者は大部分の乳酸菌にサーチュイン遺伝子が存在する事、および *L. paracasei* 3 株のサーチュインが脱アセチル化酵素活性を持つことを見いだした。これに加えて、著者は *L. paracasei* BL23 における LpSirA の標的タンパク質がタンパク質合成に関与する 30S ribosomal protein S4 であることを、世界で初めて明らかにした。更に、免疫蛍光染色により、LpSirA タンパク質は分裂細胞における分裂面と細胞極に局在する事および LpSirA-Venus 高発現株により、LpSirA タンパク質は細胞質に螺旋のような規則性をもって局在する事が観察された。以上より、著者は *L. paracasei* におけるサーチュインの役割として、タンパク質合成制御と細胞分裂に関与する事を推測した。それ故、著者はサーチュインの働きに着目することで、乳酸菌をより良いプロバイオティクスとして人々の健康増進に貢献させることができる可能性があると考えている。